UNIVERSITAT POLITÈCNICA DE CATALUNYA
BARCELONATECH
Escola d'Enginyeria de Barcelona Est

MASTER THESIS

Master in Materials Science and Engineering

DEVELOPMENT OF ALGINATE HYDROGELS FOR BONE REGENERATION

Dissertation and Annexes

Author: Mahalia Marion
Director: Carles Mas Moruno
Co-Director: Lluís Oliver Cervelló

Defense: February 2021

Resumen

El hueso es un tejido capaz de regenerarse por sí mismo después de una lesión. Sin embargo, cuando el defecto es demasiado grande, esto es imposible, y se debe utilizar un injerto de hueso. Las limitaciones asociadas a los injertos óseos tradicionales (autoinjerto, aloinjerto, xenoinjerto) limitan su uso más amplio y han llevado al desarrollo de sustitutos óseos sintéticos. Entre ellos, los hidrogeles han llamado la atención por las ventajas que aportan sus propiedades.

El objetivo de este proyecto es desarrollar hidrogeles de alginato para la regeneración ósea. A pesar de su alta biocompatibilidad y baja citotoxicidad, el uso del alginato para la regeneración ósea está limitado por su falta de afinidad celular. En consecuencia, se requiere su modificación con moléculas bioactivas. Por este motivo, otro objetivo de este trabajo es funcionalizar el alginato con péptidos RGD para mejorar la adhesión y la proliferación celular.

Los hidrogeles de alginato se prepararon mezclando alginato al 2% (w/v) con sulfato de calcio, que actúan como reticulantes y permiten la formación de estructuras 3D. La concentración final de sulfato de calcio en los hidrogeles fue del 2% (w/v). La reticulación se realizó con jeringas interconectadas, seguido de la deposición del alginato reticulado entre dos placas de vidrio separadas 2 mm. Se dejó que el alginato se reticulara durante 10 minutos y posteriormente se perforaron y lavaron los hidrogeles durante al menos 24 horas.

Para preparar hidrogeles de alginato funcionalizados con RGD, el alginato fue modifica primero con norborneno o PDEA y luego fue funcionalizado con 1 mg de péptidos RGD/g de alginato.

Los hidrogeles mostraron una estructura porosa con un tamaño de poro de alrededor de 250 µm y presentaron un alto índice de hinchazón. Su comportamiento fue el típico de un hidrogel: comportamiento de cizallamiento bajo cizallamiento y gran elasticidad. El proceso de lavado fue eficiente para eliminar el exceso de sulfato de calcio. Para la funcionalización del alginato se incorporaron 0,76 mg RGD/g de alginato, lo que representa el 76% de la cantidad introducida de péptido, lo cual refleja la eficiencia del método de funcionalización.

Estudios futuros deberían centrase en estudiar los efectos de la funcionalización en las propiedades reológicas y la estructura de los hidrogeles, así como su evaluación a nivel de adhesión celular.

Resum

L'os és un teixit capaç de regenerar-se sol després d'una lesió. No obstant això, quan el defecte és massa gran, això és impossible i s'hauria d'utilitzar un empelt ossi. Les limitacions que presenta l'ús d'empelts naturals (autoempelt, al·loempelt, xenoempelt) limiten el seu ús més ampli i han conduït al desenvolupament de substituts ossis sintètics. Entre ells, els hidrogels han cridat l'atenció a causa de de les seves propietats beneficioses.

L'objectiu d'aquest projecte és desenvolupar hidrogels d'alginat per a la regeneració òssia. Tot i la seva elevada biocompatibilitat i la baixa citotoxicitat, l'ús d'alginat per a la regeneració òssia està limitat per la seva manca d'afinitat cel·lular. En conseqüència, es requereix la seva modificació amb molècules bioactives. Per aquest motiu, un altre objectiu d'aquest treball és funcionalitzar l'alginat amb pèptids RGD per millorar l'adhesió i la proliferació cel·lular.

Els hidrogels d'alginat es van preparar barrejant alginat al 2% (w/v) amb sulfat de calci, que actuen com a reticulant i permeten la formació d'estructures 3D. La concentració final de sulfat de calci en els hidrogels va ser del 2% (w/v). La reticulació es va realitzar amb xeringues interconnectades, seguida de la deposició de l'alginat reticulat entre dues plaques de vidre separades 2 mm. L'alginat es va deixar reticulat durant 10 minuts i després es van foradar hidrogels i es van rentar durant almenys 24 hores.

Per preparar hidrògels d'alginat funcionalitzat amb RGD, l'alginat es va modificar primer amb norbornè o PDEA i després va ser funcionalitzat amb 1 mg de pèptid RGD / g d'alginat.

Els hidrogels van mostrar una estructura porosa amb una mida de porus al voltant de 250 µm i van presentar un elevat grau d'inflament. El seu comportament va ser el típic d'un hidrogel: comportament d'aprimament de cisallament i gran elasticitat. El procés de rentat va ser eficient per eliminar l'excés de sulfat de calci. Per a la funcionalització de l'alginat, es van incorporar a l'alginat 0,76 mg de RGD / g d'alginat, que representa el 76% de la quantitat introduïda i mostra l'eficiència del mètode de funcionalització

Estudis futurs harien de centrar-se en l'estudi dels efectes de la funcionalització sobre les propietats reològiques i l'estructura dels hidrogels, així com en l'avaluació de l'adhesió cel·lular.

Abstract

Bone is a tissue capable of self-regenerate after an injury. However, when the bone defect is too large, bone cannot regenerate by itself and the use of bone grafts is required. The limitations presented by the use of natural grafts (autografts, allograft, xenograft) limit their wider use and have led to the development of synthetic bone substitutes. Among them, hydrogels have attracted attention due the great tuneability of their properties.

The objective of this project is to develop alginate hydrogels for bone regeneration. Despite its high biocompatibility and low cytotoxicity, the use of alginate for bone regeneration is limited by its lack of cellular affinity. Consequently, its modification with bioactive molecules is required. For this reason, another objective of this work is to functionalize alginate with RGD peptides to improve cell attachment and proliferation.

In this work, alginate hydrogels were prepared by mixing 2% (w/v) alginate with calcium sulfate, which act as a crosslinker and allow the formation of 3D structures. The final concentration of calcium sulfate in the hydrogels was 2% (w/v). The crosslinking was performed with interconnected syringes, followed by the deposition of the crosslinked alginate between two glass plates separated 2mm. Alginate was left to crosslink for 10 minutes and afterwards hydrogels were punched and washed during at least 24 hours.

To prepare RGD-functionalized alginate hydrogels, alginate was first modified with either norbornene or PDEA and then functionalized with 1mg RGD peptides/ g alginate.

The hydrogels showed a porous structure with a pore size around 250 µm and presented a high swelling ratio. Their behavior was typical of a hydrogel: shear-thinning behavior under shear and great elasticity. The washing process was efficient to remove the excess of calcium sulfate.

For the functionalization of the alginate, 0.76 mg RGD/g alginate were incorporated in the alginate, which represents 76% of the quantity introduced, proving the efficiency of the functionalization method.

Further studies could be performed to study the effects of the functionalization on the rheological properties and structure of the hydrogels as well as to evaluate cell adhesion.

Acknowledgements

First, I would like to thank Lluís Oliver Cervelló, co-director of this project, for his constant availability and involvement, his indulgence and all the help he gave me during this project.

Thank you also to Dr. Carles Mas Moruno, director of this work, for giving me the opportunity to work on this subject and discover a type of materials and a field I did not know much about.

I would also like to thank the technical and administrative team of the Biomaterials, Biomechanics and Textile Engineering (BBT) for their support.

Glossary

Alg-**X**norb: Alginate modified with norbornene. In theory, X% of the alginate COOH groups were modified.

Alg-**X**norbg-**1mgRGDY**mgRGD: Norbornene-modified alginate functionalized with 1mg Y mg of RGD peptides.

Alg-**X**PDEA: Alginate modified with PDEA. In theory, X% of the alginate COOH groups were modified.

Alg-**X**PDEA-**1mgRGDY**mgRGD: PDEA-modified alginate functionalized with 1mg Y mg of RGD peptides.

CPC: Calcium phosphate cement.

ECMC: Extra cellular matrix.

FTIR: Fourier Transformation Infrared.

GF: Growth factor.

HG alg: Hydrogel synthetized with non-modified alginate.

HG alg-XPDEA-YmgRGD: Hydrogel made with alg-XPDEA-YmgRGD.

HG: Hydrogel.

MSC: Mesenchymal stem cell.

RGD: Arginine-glycine-aspartic acid

SEM: Scanning Electron Microscopy .

Index

Origin of the project and motivation

The market of bone substitutes has kept on increasing throughout the last decade. Following the apparition of a bone defect caused by a fracture or a pathology, a natural bone remodeling process is initiated. However, in the case of large bone defects or individuals with specific pathologies, bone cannot always heal by itself and requires external help. The main treatments currently used for bone injuries, such as autografts, allografts or xenografts, are associated with risks of infection, rejection or disease transmission, which has limited their clinical use. Synthetic bone substitutes that can provide support for bone growth and promote it are being investigated as an alternative method to traditional bone grafts. Moreover, these bone substitutes may be tuned to incorporate bioactive molecules.

Among the different types of synthetic bone substitutes considered for bone remodeling, hydrogels have shown potential due to their ability to mimic the extracellular matrix (ECM). The first part of this project will focus on synthetizing alginate hydrogels with suitable properties for bone regeneration.

Alginate is a good candidate for biomedical applications due to its biocompatibility, its low cytotoxicity and immune response, its availability and affordability. However, in its natural state, alginate has low cellular affinity, which makes it unable to promote cell adhesion and bone regeneration. To overcome this limitation, functionalization with peptides is a powerful way to improve cellular attachment on alginate. The second part of this report will investigate different strategies to incorporate peptides on the alginate backbone.

1. State of the art

1.1. Bone

1.1.1. Bone structure and composition

Bone belongs to the family of hard tissues, like tooth enamel or dentin. This dense tissue is a mineralized tissue composed of an extracellular matrix (ECM), which provides the cells with the perfect environment to perform their functions. Three main components can be found in the ECM. The organic phase, which accounts for 20-25% of bone weight, and it is mainly composed of type I collagen. Type I collagen serves as a framework for bone cells, maintains bone strength and promotes bone formation [1]. The inorganic phase, made of calcium phosphate, represents 65% of the bone weight. The 10% remaining is water, essential for the mechanical properties of bone [1], [2]. Regarding bone structure, two different parts are distinguished: cortical and trabecular bone. The cortical bone is the hard, outer layer, while the cancellous bone is the internal tissue and is light and porous and with high biological activity [2] [3].

1.1.2. Bone cell types

Bone is made up of three types of cells: osteoblasts, osteocytes and osteoclasts. Osteoblasts are bone-forming cells responsible for the synthesis, secretion and mineralization of bone during bone formation and remodeling process. They are derived from mesenchymal stem cells (MSCs). MSCs are star-shaped cells that can differentiate into a variety of cell types including osteoblasts, chondrocytes, fibroblasts, myocytes and adipocytes [4]. Osteocytes are inactive post-synthetic osteoblasts that have been entrapped in the bone matrix they produced during the mineralization process. Osteoclasts are responsible for bone resorption via enzymatic secretion, such as acid phosphatase that dissolves the collagen and the inorganic phase of the bone [2] [3].

1.1.3. Bone remodeling process

The bone remodeling process takes place in several phases, as summarized below in Figure 1: activation, resorption, reversal, formation and mineralization phases. Bone reconstruction starts by the differentiation of lining cells into osteoclasts. Various events can trigger this differentiation: a micro-fracture or any change in the mechanical loading exerted on the bone, the release of factors in bone environment… After their differentiation, osteoclasts adhere on bone surface and they start the bone dissolution process. To avoid excessive bone resorption, osteoclasts undergo apoptosis once they have played their role. Reversal cells intervene at this step to remove the waste produced during bone

degradation. The resorption of bone matrix initiates the release of growth factors (GFs), which will in turn activate the formation of new bone matrix by osteoblasts. The mineralization of this bone matrix completes the bone remodeling process [4].

The capacity of bone to self-regenerate following an injury is possible due to its high vascularization, unlike cartilage, which cannot self-heal [5]. However, there are clinical cases in which bone fails to self-repair. For instance, tibia fractures are particularly prone to this problem: "up to 13% of fractures occurring in the tibia are associated with delayed union or fracture non-union" [6]. Bone regeneration impairment is more likely to happen in cases where the regenerative process is hindered by an anomaly, such as necrosis, osteoporosis or infection, or when bone defects are larger than a critical size.[2], [5].

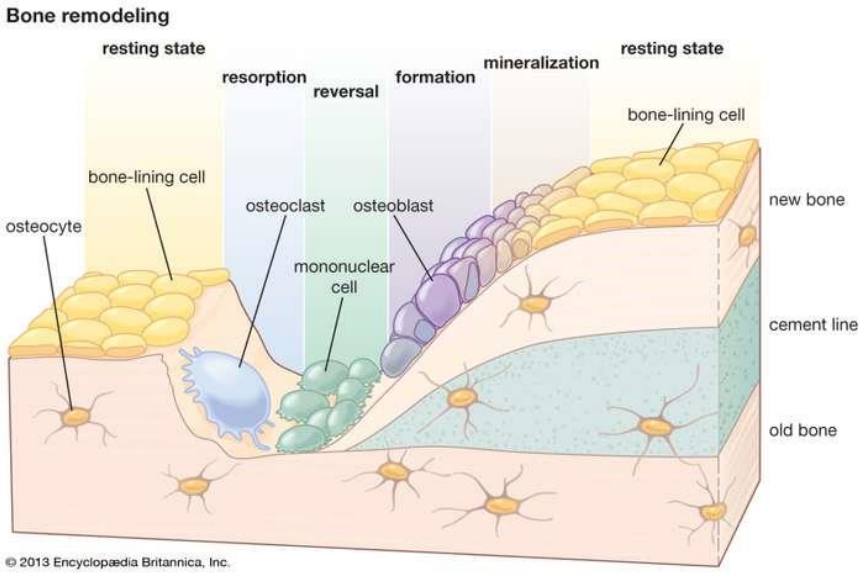

Figure 1: Bone remodeling process [3].

1.2. Bone grafts

Alternative bone remodeling solutions are sought when bone self-healing fails. Bone transplantation is one of the most performed procedures after blood transfusion [7]. Natural or synthetic bone grafts can be used. In either case, good integration between the replacement material and the natural tissues is required for efficient bone regeneration and to avoid unwanted immune responses [2]. An ideal bone graft material should have good osteoconduction, osteoinduction, osteointegration and osteogenesis [7].

Osteoconduction refers to the capacity of a material to promote migration of bone cells into the graft and support bone growth on its surface and within its pores. Osteoinduction is the ability of a bone graft to recruit MSCs and to stimulate their differentiation into osteoblasts. Osteointegration characterizes the interaction between bone tissue and the implant and its ability of that bone tissue to grow on the implant without the formation of a fibrous tissue layer. Finally, the osteogenesis is the capacity of a graft to produce new bone material [7]–[9].

Furthermore, ideal bone scaffolds should meet the following requirements:

- → Biocompatibility to avoid adverse immune reactions.
- → Structural, physio-chemical and mechanical properties similar to those of natural bone tissues.
- → Favorable environment for cell adhesion, proliferation, migration and differentiation.

Controlled rate degradation, similar to the rate regeneration of new tissues is another important parameter to control in the development of a biomaterial. Normally, the scaffolds should be stable for around 10 to 16 weeks, but it varies depending on the patient condition and the type of injury. [5]

1.2.1. Natural bone grafts

Bones harvested from humans or animals can be used as scaffolds to promote and guide bone remodeling. Three main types of natural bone grafts exist: autografts, allografts or xenografts.

Autografts (autologous) are bone transplants within the same patient and are usually harvested from the iliac crest. They are preferred to allografts and xenografts for their osteoinduction, osteoconduction and osteogenesis capacities, but the extraction of this kind of graft is painful for the patient and local complications can arise on the donor site [10], such as morbidity. Chronic donor site pain is reported to happen in 10 to 50% of autograft transplantation cases [7]. In addition, autografts are not appropriate for massive bone defects due to their limited availability.

Allografts are commonly used in orthopedics. They are also obtained from human bones except they do not come from the patient but from a donor. They usually are harvested from cadavers, but they can also be from living patients, like the ones undergoing total hip replacement. Allograft bones are preserved through freeze-drying or freezing techniques [11] and lose most of their strength and osteogenic potential during the processing. For that reason, other osteoconductive agents might need to be used simultaneously [12]. Compared to autografts, allografts are more available and they do not have the risks of donor site morbidity [7]. Although they have shown clinical success, many complications can arise following an allograft transplant, such as rejection or transmission of diseases. In massive allograft surgeries, infection rates can reach 20%. Moreover, in case of infection, the graft removal and the administration of antibiotic treatments are necessary. If the infection persists despite the measures taken, it can lead to amputation or even death [13].

Xenografts come from animals, usually from porcine or bovine origin [14], and are primarily used for spinal and maxillofacial applications. Their availability and acceptable osteoconduction play to their advantages [7]. However, they are subjected to the same type of complications as allografts including pathogen transmission, immunogenic rejection and prolonged graft integration [10].

1.2.2. Synthetic bone grafts

Other materials than bone can be used to replace the damaged bone or to help its regeneration. This is the case of synthetic bone substitutes, such as ceramics, metals, or polymers. The main advantage to synthetic bone grafts compared to natural ones is that their properties can be tailor-made depending on their application.

Bioceramics are extensively used as synthetic bone grafts. They can be classified according to their silicate content and chemical composition (see Figure 2). There are some evidences suggesting that silicates play a key role in bone formation [15]. The first bioceramics used in bone tissue engineering were hydroxyapatite and β-tricalcium phosphate, obtained by sintering the ceramic at high temperature. Later, calcium phosphate cements (CPCs), which do not require sintering, were introduced. CPCs are widely used in bone tissue engineering nowadays, as their composition and structure is close to those of bone. One of the advantages of CPCs is that they can set in situ and be loaded with drugs and bioactive molecules as their setting reaction is not exothermic. Moreover, CPCs are bioactive, biodegradable and osteoconductive. They typically have high porosity, which promotes vascularization and osseointegration. However, they have lower mechanical strength compared to natural bone, which limits their use in load-bearing applications. Other common bioceramics used as bone grafts include calcium sulfate ceramics and bioactive glasses [16]–[18] .

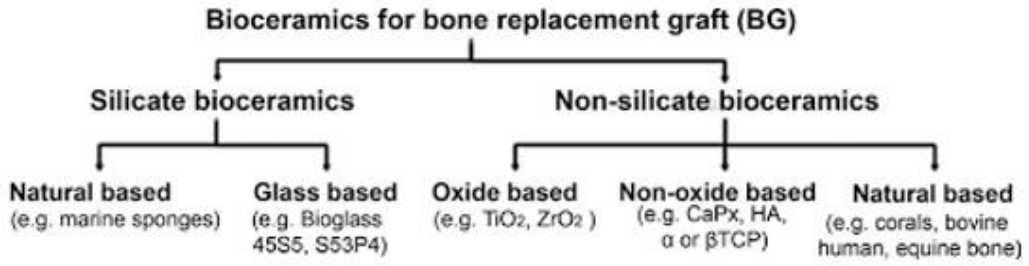

Figure 2: Classification of bioceramics for bone replacement according to their composition [15]

Metals such as tantalum, titanium, iron or magnesium, and their alloys, are used as bone implants, most often in orthopedics and dentistry. Thanks to their high mechanical strength and fracture

toughness, metals are ideal for load-bearing applications. They are usually not intended to be resorbed and corrosion, that could cause the metals to degrade, is undesirable. They are bioinert, which reduces the immune response and the reaction to foreign bodies. However, their lack of bioactivity also means they do not actively participate in bone regeneration [19]. Metallic implants are also prone to stress-shielding, due to their high stiffness compared to the one of bone. During this process, when stress is applied to a bone containing a stiff implant, most of the stress will be transmitted to the implant, decreasing the loading on the bone, which may finally result in bone resorption [20], [21]. Nitinol, a nickel-titanium alloy, has shown potential as a bone graft due to its similar mechanical properties to the ones of bone [22].

A wide range of polymers is also used for bone replacement. Polymers can be intended to degrade by hydrolysis or erosion, leaving free space for newly formed bone. Thus, bone is able to regenerate without any foreign body remaining. Non-degradable polymers are used to fill defects when bone is unable to self-regenerate. Polymers can also be used in the form of hydrogels [23].

1.3. Hydrogels for bone regeneration

1.3.1. General properties of hydrogels

Hydrogels are 3-dimensional polymeric networks that are able to retain large amount of water [24], [25]. They have shown strong potential for bone tissue engineering thanks to their softness and their ability to retain high-water content [25]. If their polymer source is well chosen, they can be biocompatible and biodegradable [2]. Biocompatible is said of a material that can be used in a biological medium without having a negative effect on it.

One of the greatest advantages of hydrogels as bone substitutes is their tunable properties. By adjusting hydrogel composition, the properties can be tailored to mimic the mechanical strength and the structure of the natural ECM, thus facilitating cell adhesion, osteogenic differentiation, and integration with the surrounding tissues.

Their porous framework allows the diffusion of nutrients, oxygen, and metabolic waste, which makes hydrogels excellent candidates to encapsulate proteins and other regenerative molecules within their mesh and control their release over time. The pore size can be adjusted with the hydrogel's composition and synthesis process [26]. Porosity is also important for vascularization and ingrowth of new tissue.

Hydrogels can also be made into a wide variety of shapes and sizes. For a minimally invasive procedure, they should ideally be injectable to directly fit the bone defect. In this way, surgery and its potential

complications are avoided, the pain of the patient is reduced, and the administrative process is lightened.

Finally, depending on their chemical structure and their nature, they can undergo enzymatic or hydrolytic degradation to free space for new bone formation [5], [25].

1.3.2. Polymer sources for hydrogel synthesis

Both synthetic and natural sources of polymers are used to synthetize hydrogels. The selection of the hydrogel source will depend on the application. It is also possible to combine both types of hydrogels to have biomaterials with the advantages of natural and synthetic polymers.

Natural polymers

Natural polymers used for hydrogels are usually found within the human body, and thus show high biocompatibility and low immune response and cytotoxicity (toxicity to cells). Most of them also promote cell adhesion, proliferation and new tissue formation. However, their physicochemical properties are hard to control and they may vary from one batch to another. Two families of natural polymers are used: polysaccharides (alginate, cellulose, hyaluronic acid, chitosan…) and proteins (collagen, gelatin, fibrin…). Table 1 summarizes the most used natural hydrogels and their main characteristics. (see Table 1) [2], [5].

Table 1: Overview of the main natural polymeric sources for hydrogel synthesis.

Natural polymers	Polysaccharides	Alginate	Derived from brown algae. Alginate hydrogels are used for various tissue engineering applications and for protein delivery.
		Cellulose	Main component of the cell wall of plants, including wood. Biomedical applications of cellulose hydrogels include wound healing and tissue engineering.
		Hyaluronic acid	One of the main components of ECM. It is mainly found in skin, connective tissues and eyes. It plays an important role in tissue regeneration and inflammation response. Used in bone and cartilage regeneration.
		Chitosan	Linear polysaccharide derived from natural chitin. Chitin can be found in the exoskeleton of arthropods such as crustaceans and insects, in fish scales… Chitosan-based hydrogels can be great cartilage substitutes.

	Proteins	Collagen	Most abundant protein in mammals. It is mostly present in connective tissues such as bones, cartilage, skin, tendons and ligaments. Dozens of different types of collagen exist, type I and II being the ones most often used in hydrogels. Collagen-based hydrogels are used as cartilage substitutes.
		Gelatin	Obtained by hydrolyzation of collagen.
		Fibrin	Protein appearing in blood during coagulation. It is obtained by polymerization of fibrinogen.

Synthetic polymers

Contrarily to natural polymers, synthetic polymers have uniform properties, are long-lasting and present better mechanical properties. Their properties like porosity, degradation time or mechanical properties. For example, poly(lactic acid) (PLA) and poly(D,L-lactide-co-glycolide) (PLGA) have shown tunable physicomechanical properties, and a tunable degradation rate in the case of PLGA [2], [27]. Synthetic polymers also have great potential for delivering bioactive molecules [2].

On the other hand, their lower biocompatibility and acid byproducts might negatively influence in the regeneration of bone tissue [5]. For better cell adhesion, improved mechanical strength and controlled properties, a combination of natural and synthetic polymers can also be envisaged [24].

Main synthetic polymers used nowadays include polyethylene glycol (PEG), polyvinyl alcohol (PVA), polyacrylamide (PAM), polylactic acid (PLA) and polypeptides [2], [5], [24].

Table 2: Overview of the main synthetic polymeric sources for hydrogel synthesis.

Synthetic polymers	PEG	Although PEG is bioinert and does not have any adhesive properties, it can easily be functionalized with bioactive molecules.
	PVA	Hydrophilic polymer. PVA-based hydrogels are very similar to cartilage in terms of permeability, physical and mechanical properties and water content.
	PLA	Biodegradable and biocompatible polymer. PLA with low molecular weight is preferred for tissue engineering applications due to its higher degradation rate. [28]

1.3.3. Crosslinking methods of hydrogels

Hydrogels can be either physically or chemically crosslinked to form a three-dimensional network.

In the case of physical crosslinking, no crosslinker is needed, as the network is formed by forces such as molecular entanglements, hydrophobic interactions, ionic or hydrogen bonding (see Figure 3a). They can be triggered by changes in pH, temperature, stress or ionic concentration, such as the ionic crosslinking. This type of crosslinking is considered reversible as the network can be dissolved by reversing the environmental conditions to their initial state [29].

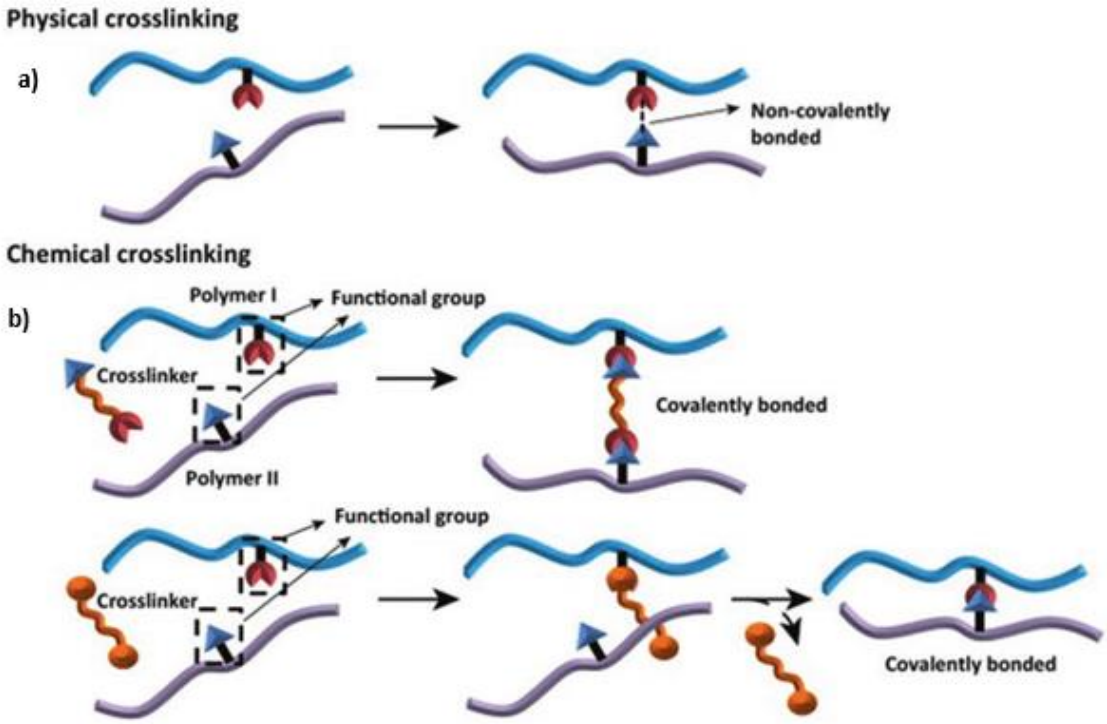

Figure 3: Mechanism of: a) physical crosslinking and b) chemical crosslinking [30]

Chemical crosslinking involves a chemical process, in which hydrogel networks are covalently bonded (see Figure 3b). Some examples of chemical crosslinking are enzymatic crosslinking, click crosslinking (Schiff-base reaction, Michael addition) and photo crosslinking [31]. Enzymatic crosslinking is highly selective for a specific enzyme and can be achieved under mild conditions [32]. Click chemistry refers to a wide range of reactions with high yield and creating highly selective products. Schiff-base crosslinking and Michael addition are some examples of click chemistry reaction used to synthesize hydrogels. In the first case, Schiff bases react reversibly in mild conditions, allowing for self-regenerating hydrogels [33] while in Michael addition, there is the nucleophilic addition of a carbanion or a nucleophile to an α,β-unsaturated carbonyl compound. Like Schiff-base reactions, Michael-type additions can take place in very mild conditions. In photo crosslinking, a liquid monomer or macromer containing a photo initiator is crosslinked under light by free radical polymerization. The polymerization is fast: from less than a second to a few minutes. If the polymerization has to be carried out with living cells, the light energy and the amount of photo initiator should be reduced to avoid damaging the cells [32], [34].

1.3.4. Loading of hydrogels

In the case of small fractures where the damaged tissues have good healing potential, bared polymeric hydrogels can be used as supportive scaffolds to promote the formation of new bone tissue. However, in many of the cases where the bone does not heal by itself, using bared hydrogels is not enough for complete bone regeneration. This happens mainly if the tissues have poor regenerative capacities and in large fractures. The incorporation of cells and biological molecules helps tissue regeneration and speeds up the healing process. The controlled and localized release of those regenerative agents depends on the intrinsic properties of the hydrogels [5].

Different types of loading exist. In direct loading, cells and biomolecules are directly added in the hydrogels, either prior to the gelation by mixing them to the precursor solutions or via absorption after the gelation. Their release is dictated by the diffusion of the biomolecules and the degradation of the hydrogels. However, in indirect loading, the regenerative molecules are incorporated into micro or nanoparticles distributed within the hydrogel network [5].

Most commonly used regenerative molecules include growth factors (GFs). GFs are bioactive molecules naturally secreted by cells and tissues. They act as signaling molecules between cells and they are responsible for cell growth, differentiation and tissue healing, among others. GFs are divided into families, which have different properties and functions. For example, bone morphogenetic protein 2 (BMP-2), which belong to the transforming growth factor-β (TGF-β) family, stimulate osteogenic differentiation, while vascular endothelial growth factors (VEGFs) are angiogenic factors that are responsible for new blood vessel formation [35].

Cells can also be added to hydrogels, but their regenerative capacity varies depending on the kind of cells is used. For instance, the use of osteocytes is frequent in bone regeneration although their use is limited by the scarcity of their supply sources. Adult stem cells, such as MSCs, are interesting due to their capacity to differentiate into different specific cell types. Embryonic stem cells are also capable of differentiation and their plasticity might permit more integrative and extensive repair. They have shown good clinical success. However, their potential is limited due to safety and ethical reasons [35].

1.4. Alginate-based hydrogels

1.4.1. Alginate for hydrogels

Generalities

Alginate is a polysaccharide extracted from brown algae [31], a seaweed that grows in temperate areas [36]. Alginate is composed of D-mannuronic acid (M-blocks) and L-guluronic acid (G-blocks). These

blocks contain hydroxyl and carboxyl groups [37] (see Figure 4). The source of the alginate impacts directly the block distribution, its proportions of M and G-blocks, and consequently, its properties. M blocks are linear, have a flexible conformation and participate in the immunogenic nature of alginate. On the other hand, the rigid structure of G-blocks hinders sterically the carboxyl groups of alginate and gives its stiffness to the molecular chains [25]; longer G-blocks will result in alginate hydrogels with higher mechanical strength. Research suggests that only G-blocks intervene in crosslinking with divalent cations [38].

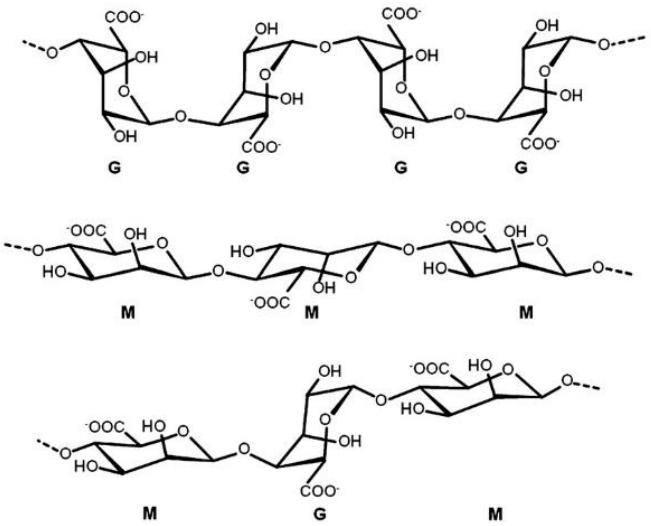

Figure 4: Chemical structure of G-block, M-block and alternating block in alginate [38].

Alginate dissolves in water to form a viscous solution [36]. Alginate solution is a non-Newtonian fluid, which means that it gets more viscous for decreasing values of pH. It reaches its maximum viscosity for pH around 3-3.5. The sensibility to pH is due to the carboxyl groups present on the alginate backbone. The swelling ratio of alginate increases with the pH because of the protonation of those carboxylate groups [25], [38].

Advantages

Alginate is one the most-commonly used hydrogels for bone tissue engineering (and other biomedical applications, like bioprinting) [25]. Reasons for this are its biocompatibility and non-toxicity, its high availability that makes it affordable and its good gelation. Moreover, the fabrication process is very flexible and allow tailing alginate properties [5], [31].

Depending on their composition, alginate-based hydrogels can gel in situ, which means they are in sol form before the injection in the body and crosslink under physiological conditions. This allows the use of alginate as injectable hydrogels, with the main advantage of being minimally invasive. Another important aspect is the alginate purity, as it might influence its biocompatibility and toxicity.

Limitations

The principal limitation of alginate in bone tissue engineering is its low cell affinity. As it does not have any sites for cell attachment, it does not interact well with proteins and cells [39]. While proteins can be adsorbed onto alginate hydrogels thanks to the hydrophilicity of alginate, cells are usually unable to attach themselves. Hence, on its own, an alginate hydrogel is unable to promote cell attachment, migration and proliferation. However, the combination with other polymers like hyaluronic acid [40] or the functionalization with peptides can compensate its lack of bioactivity. The functionalization of alginate will be further developed in a later section.

Alginate is also limited in its use by its poor degradation, slow and incomplete. Most commercially available alginates also have high molecular weight. Although higher molecular weight can improve the mechanical properties, the subsequent increase of viscosity is detrimental to its manipulation[25], [38]. It also lacks structural stability, especially as an injectable hydrogel, due to its relatively low mechanical properties (compressive modulus = 1-8kPa) [5]. However, it can be combined with other types of biomaterials to obtain higher mechanical properties [31].

Lastly, the properties of alginate are largely affected by its composition and degree of purity.

1.4.2. Crosslinking methods for alginate hydrogels

Ionic crosslinking

Ionic crosslinking is the most frequent method to prepare alginate hydrogels. Ionic crosslinkers, usually divalent cations, are mixed with alginate solution. Ca^{2+} ion is the most commonly used, but any other divalent cation works, except for Mg^{2+} may be also used. Affinity of the alginate towards divalent cations reduces in the following order: Pb>Cu>Cd>Ba>Sr>Ca>Co, Ni, Zn>Mn [41].Trivalent cations like Al^{3+} or Fe^{3+} have also been used [42].

When crosslinking agents react with the alginate monomer, ionic bonds are formed. The interactions with M-blocks are weak, but cations are tightly bound with the carboxylate groups of the G-blocks [25], [38]. The gelling mechanism between G-blocks is known as the egg-box model, as it forms a junction area shaped like an egg-box (see Figure 5) [36], [43]. Calcium chloride ($CaCl_2$) is extensively used for alginate crosslinking. However, it is highly soluble in aqueous solutions, which makes its gelation rapid and difficult to control. Alternatively, calcium sulfate ($CaSO_4$) and calcium carbonate ($CaCO_3$), that are less water soluble, can be used for a more controlled gelation. The use of phosphate-based retarding agents, such as $NaPO_3$ [42] or Na_2HPO_4 [26], can also be envisaged. With slower gelation rate, the hydrogel is manipulable for longer time, thus better mixing and injectability can be achieved. However,

a good compromise between the quality of the mixing and the gelation time must be found, as the crosslinking should still be fairly quick.

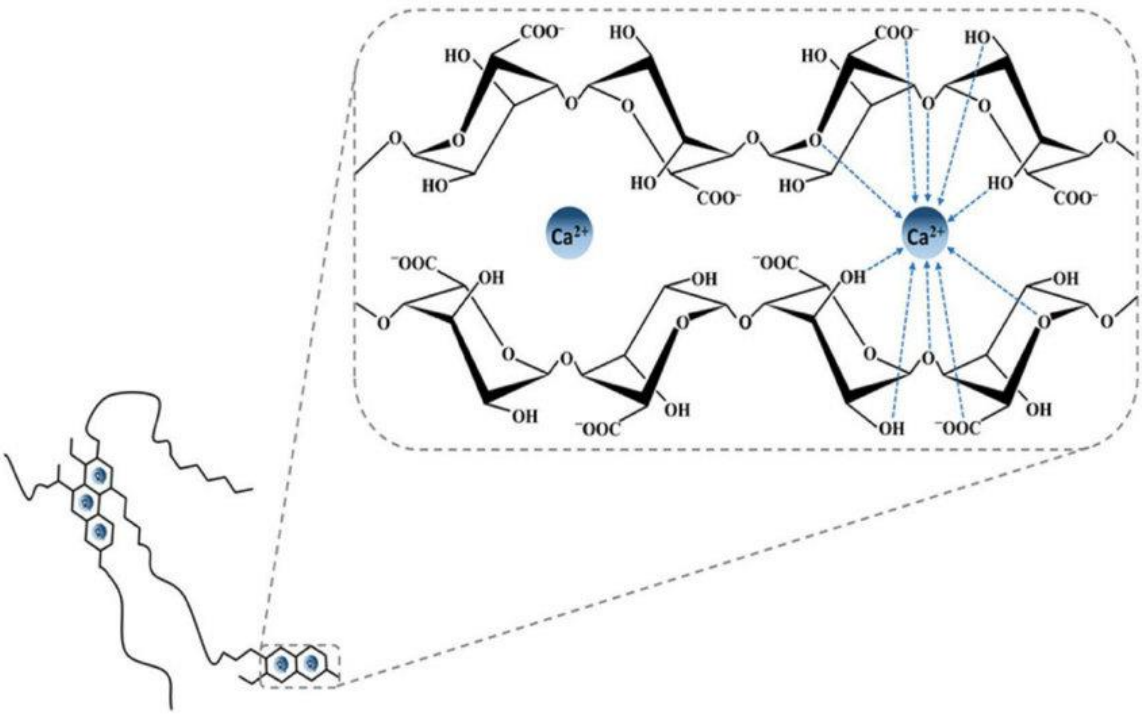

Figure 5: Egg-box model representing the interactions between G-blocks and calcium ions during ionic crosslinking [43].

Other crosslinking methods

Another crosslinking method for alginate hydrogels is covalent crosslinking. Covalent crosslinking can be performed through the intermediary of crosslinking molecules, photosensitive agents or under the action of enzymes, among others. By using covalent crosslinking, it is possible to improve the stability and the mechanical properties of hydrogels. However, it usually requires a backbone modification of the alginate beforehand [41], [44].

1.4.3. Alginate modification and functionalization

Alginate modification and functionalization are performed in order to induce cell interaction and to improve or transform its physiochemical properties. The carboxylate groups of the monomer backbone can be easily modified to attach other groups or molecules such as peptides or fluorescence markers on the alginate structure [44]. The difference of reactivity between the hydroxyl and carboxyl groups of the alginate allows chemo selective reactions involving only either the carboxyl or the hydroxyl groups [37].

Improving cell adhesion of alginate hydrogels is crucial for bone regeneration applications. One of the main limitations of alginate is its poor cellular affinity: cells do not interact well with alginate and consequently, alginate-based hydrogels do not stimulate cell adhesion and proliferation. To promote cell adhesion and growth, peptides containing the RGD sequence in particular have been extensively used to functionalize alginate [5], [45]. RGD sequence (see Figure 6) is a tripeptide composed of arginine, glycine and aspartic acid. This peptide is recognized by integrins (cellular receptors responsible of cell adhesion). Once alginate is modified with RGD, it will increase cellular attachment and viability. For instance, in Bubenikova's work [46], cell viability was very low in the case where no peptides were added to the alginate. However, the addition of a sufficient amount of RGD peptides (14.40 mg RGD/g alginate) increased the cell viability. The minimum concentration of RGD peptides required for having a cellular response probably depends on the type of cells. For example, it was reported that 12.5 µg/mg alginate are required for supporting the adhesion for MCT3-E1 cells and 10µg/mg alginate for C2C12 [38].

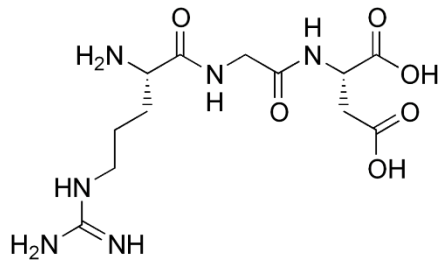

Figure 6: RGD motif (Arginylglycylaspartic acid) [47].

The most common way to functionalize alginate with peptides is by carbodiimide chemistry. Rowley and al. [48] functionalized alginate with RGD peptides using aqueous carbodiimide chemistry. They used 1-ethyl-(dimethylaminopropyl)carbodiimide (EDC), a water-soluble carbodiimide, to form amine bonds with the carboxylate groups present on the alginate backbone. N-hydroxy-sulfosuccinimide (sulfo-NHS) was afterwards introduced to stabilize the reactive intermediate formed and increase the efficiency of the amine bond formation. GRGDY peptide was finally attached to the alginate through the terminal anime of the sequence.

Besides peptides containing a terminal amine, thiol terminated RGD motives can also be used. In Bubenikova et al. [46], alginate was activated with EDC and sulfo-NHS. Then, 2-(2-pyridyldithio)ethyleneamine (PDEA) was introduced to allow a thiol-disulfide exchange reaction with the thiol-terminated peptides (see Figure 7). Another option is the use norbornene to modify the carboxylic groups of alginate. A photo initiator and thiol- containing peptides are then added to the previously norbornene-modified alginate. The alginate functionalization with the peptide is done by exposing the mixture to UV light (see Figure 8).

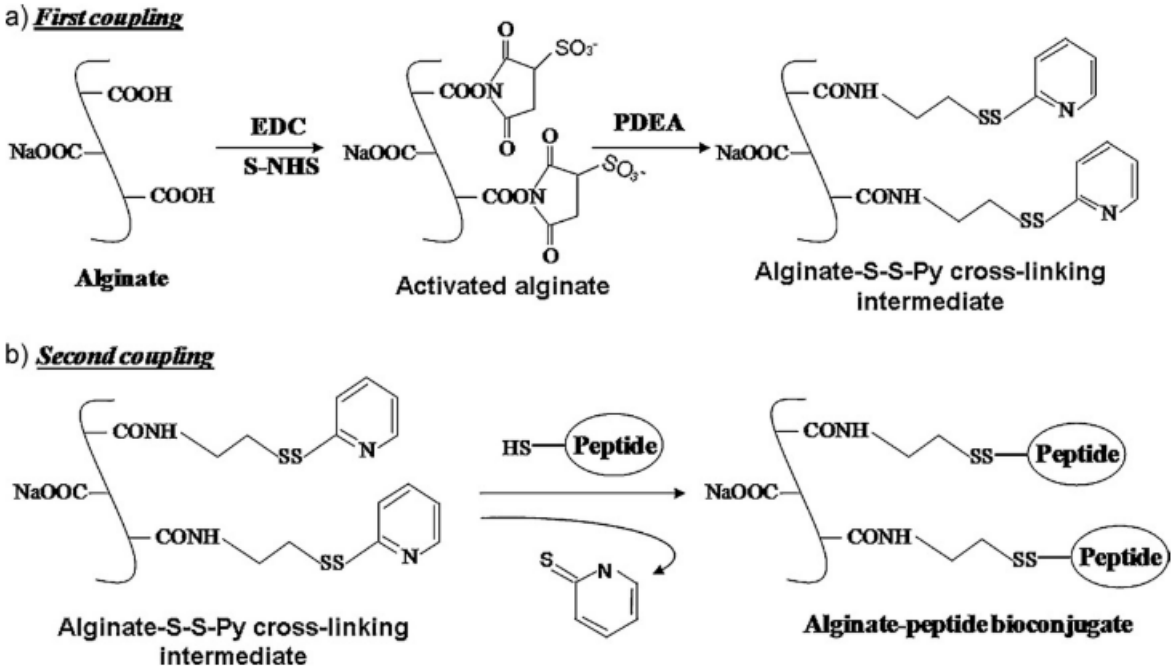

Figure 7: Reaction scheme of the (a) alginate modification with PDEA and (b) thiol disulfide exchange between the PDEA-modified alginate and the thiol-terminated peptides [46].

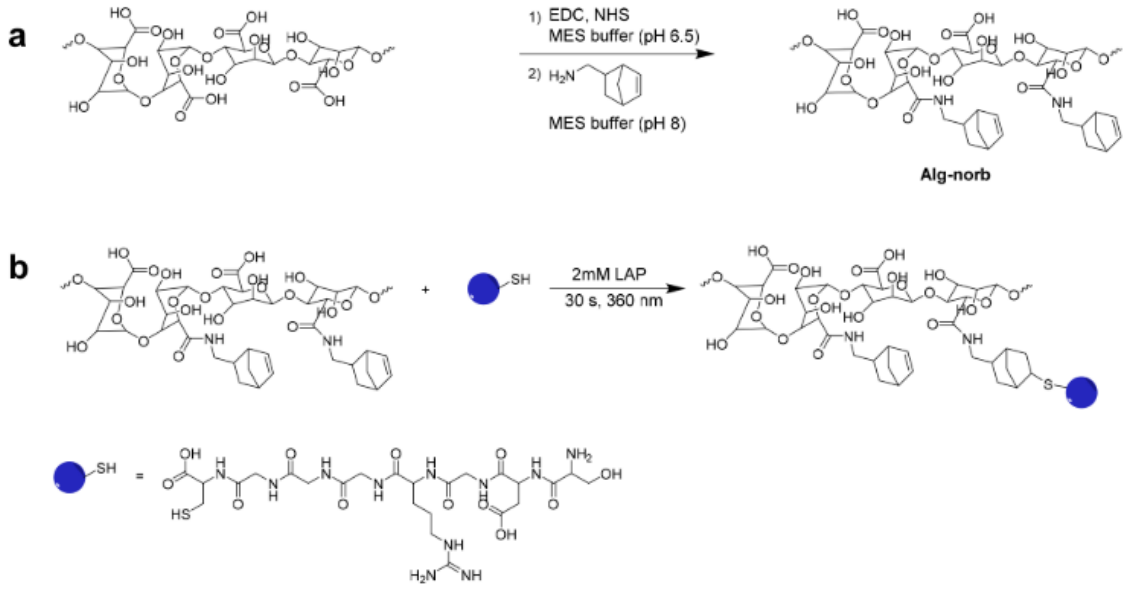

Figure 8: Reaction scheme of the (a) alginate modification with norbornene and (b) photoinitiated thiol-ene conjugation of peptides with the norbornene-modified alginate [49].

An alternative to carbodiimide chemistry is the oxidation of alginate, followed by its amination. Dalheim et al. [39] first added sodium(meta)periodate ($NaIO_4$) to an alginate solution to oxidize the

alginate. The quantity of $NaIO_4$ used for modifying the alginate varied according to the desired degree of oxidation. Then, a reductive amination was carried out by mixing the periodate oxidized alginate with peptides.

Alginate can also be functionalized once the hydrogels have already been formed. Rowley and al. [48] ionically crosslinked an alginate solution with $CaSO_4$. The hydrogel disks formed were then centrifuged in a solution containing EDC, sulfo-NHS and peptides.

Alginate modification can be performed to modify other properties. For example, He et al. [50] improved the biodegradability of alginate through periodate oxidation, whereas Lueckgen et al. [51] incorporated a specific enzymatically-degradable sequence by using carbodiimide chemistry and norbornene.

2. Objectives

This project is divided in two main parts. The first one will focus on the development of alginate hydrogels and the second one to engineer a protocol to functionalize alginate with RGD peptides. The idea is to use these hydrogels to perform cell assays, which is way they have to be functionalized. However, the cell assays are part of another project and will not be discussed here.

Based on that, this work has three main objectives:

2.1. Synthesis and characterization of alginate-based hydrogels

→ Determination of the composition of the hydrogels
→ Implementation of a protocol to synthetize the hydrogels
→ Physicochemical characterization of the hydrogels (SEM, rheology, swelling test)

2.2. Optimization of the fabrication protocol of hydrogels

→ Improve the homogeneity of the hydrogel disks
→ Improve the reproducibility of the protocol

2.3. Functionalization of alginate

→ Functionalization of alginate with norbornene
→ Functionalization of alginate with PDEA
→ Physiochemical characterization of the hydrogels made with functionalized hydrogels (rheology)
→ Characterization of alginate to see if it is well functionalized (FTIR, fluorescence test)
→ Determination of the protocol of functionalization that works the best

3. Materials and methods

3.1. Materials

Sodium alginate (BioChemica) with a molecular weight ranging between 10000 and 60000 g/mol, calcium sulfate hemihydrate 98% (Sigma-Aldrich, $CaSO_4 .½H_2O$) and sodium hexa-meta phosphate (Panreac, $(NaPO_3)_6$) were used for the hydrogels. 1-ethyl-(dimethylaminopropyl)carbodiimide (EDC, Sigma-Aldrich), N-Hydroxysuccinimide (Sigma-Aldrich, NHS), 5-Norbornene-2-methylamine (TCI Chemicals, norbornene), 2-(2-Pyridyldithio)ethyle-neamine (MesChemExpress, PDEA) and lithium phenyl(2,4,6- trimethylbenzoyl)phosphinate (Sigma-Aldrich, LAP) were used for the functionalization of the alginate. 2-(N-Morpholino)ethanesulfonic acid sodium salt (<99%, Sigma-Aldrich, MES sodium salt) and sodium chloride (<99%, Sigma-Aldrich, NaCl) were used to prepare the MES buffer. Spectrum™ Spectra/Por™ 3 RC Dialysis Membrane Tubing 3500 Dalton MWCO was used for the dialyses.

Peptides containing a RGD sequence were used. The peptide used for most of the assays was MPA-(Gly)3-RGDS-OH (Mw=692.25 g/mol). A second peptide with a fluorescent molecule (see Figure 9) was used: CF-RGDS-(Ahx)3-C-OH (Mw=1233.5 g/mol).

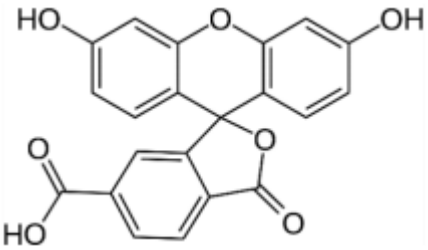

Figure 9: Chemical structure of the CF molecule.

3.2. Hydrogels preparation

3.2.1. Optimization of the composition of hydrogels

Alginate hydrogels were synthesized through ionic crosslinking. To get an idea of the optimal composition of the hydrogels, sodium alginate solutions at various concentrations were combined with two different crosslinkers, also in varying concentrations. The concentrations tested were based on experiments documented in the literature. The concentration of the sodium alginate solution varied from 0.25% to 4% and two calcium-based ionic crosslinkers, $CaCl_2$ and $CaSO_4$, were tested with final concentrations in the hydrogels ranging from 10 to 500 mM (see Figure 10).

Stock solutions of calcium chloride were prepared in advance for practicability, as calcium chloride dissolves easily in aqueous solutions. On the other hand, calcium sulfate has a low solubility in water and precipitates quickly, which did not allow their preparation beforehand. Also, two different stock solutions of $CaSO_4$ were prepared: 1.22M and 3M $CaSO_4$ stock solutions were prepared just before use, and adequate volumes of those solutions were taken to obtain the chosen concentration in the hydrogels. When using a 3M solution, the volume injected is smaller and changes less the total volume of the hydrogel but is expected to dissolve less well since it is more concentrated. The specific concentration 1.22M was chosen as it was often used in the literature [26], [42].

In the following experiments, 2% (w/v) sodium alginate solution and crosslinking was performed with the 1.22M $CaSO_4$ stock solution. The final $CaSO_4$ concentration in the hydrogels was 2%(w/v) (60mM).

Different concentrations of the retarding agent $(NaPO_3)_6$ were tested. In the literature, concentrations used ranged from 0.2% to 12% (w/v) [26], [42]. Here, the concentration used were 0.02%, 0.2%, 1% and 2% (w/v). By slowing down the crosslinking of the hydrogel, it eases the fabrication process. The mixture can be manipulated for a longer time before gelation, allowing better mixing and shaping. It also helps the dissolution of $CaSO_4$.

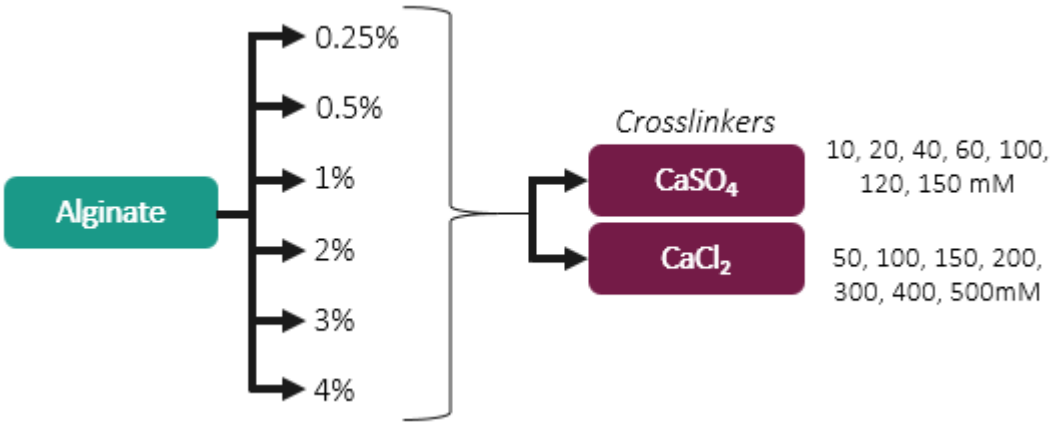

Figure 10: Compositions tested for the hydrogels

3.2.2. Fabrication protocol of the hydrogels

Protocols 1 and 2

The protocol to prepare the hydrogels was adapted from the work of Dhoot et al [42]. Hydrogels containing 2% (w/v) of alginate and 2% (w/v) of $CaSO_4$ were prepared. A 2% (w/v) alginate solution was prepared by dissolving alginate powder into a 0.02% (w/v) $(NaPO_3)_6$ buffer. To allow the complete dissolution of the alginate, they were kept under magnetic stirring at 800 rmp, overnight and at room temperature. The solution was the transferred to a 50 mL falcon tube. $CaSO_4$ was dissolved into 1 mL of distilled water in an Eppendorf tube to obtain a 1.22M stock solution. $CaSO_4$ was dissolved by quickly shacking the Eppendorf and thoroughly using a vortex mixer. 984 µL of that $CaSO_4$ stock solution were injected into the falcon tube containing the alginate solution to obtain a $CaSO_4$ final concentration in the hydrogel of 2% (60mM). The tube was shaken vigorously by hand for about 15 seconds.

(**Protocol 1**) The mixture was immediately poured into a 9 cm-diameter glass Petri dish and was covered with a smaller 8 cm-diameter dish to obtain smooth surfaces and allowed to gel for 2 hours at room temperature. After complete gelation, 10 mm-diameter by 3mm thick disks were cut using a hollow metallic cylinder.

(**Protocol 2**) The mixture was left to crosslink between two glass plates separated by 2mm spacers to improve the shape homogeneity of the hydrogels.

Protocol 3

The following protocol was implemented to improve the homogeneity of the crosslinking of the hydrogels. Alginate (bulk or peptide-modified) was dissolved into dH_2O at a concentration of 2% (w/v). 10 mL of that solution were taken with a syringe. 1.22M $CaSO_4$ and $(NaPO_3)_6$ were injected in another syringe. The volumes injected were so that the final concentrations in the hydrogels are 60 mM $CaSO_4$ and 3 mM (0.2% w/v) $(NaPO_3)_6$. The air in both syringes was carefully removed to prevent the formation of air bubbles in the hydrogels. The syringes were connected, and their content was quickly mixed 30 times. The mixture was injected between two glass plates separated by 2mm spacers and was left to crosslink. After 10 min, hydrogels disks were cut with two different dimensions (Ø:14 mm, t:2mm or Ø:8 mm, t:2mm) depending on their intended use. The hydrogels prepared with alginate functionalized with PDEA and RGD peptides were left to crosslink for 20 min instead of 10 min.

The material used for the hydrogels synthesis is shown in Figure 11, and the Table 3 below shows the main difference between each fabrication protocol.

Table 3: Differences between the three fabrication protocols of hydrogels.

	Composition			**Processing**		
	Alginate	*$CaSO_4$*	*$(NaPO_3)_6$*	*Mixing by ….*	*Left to crosslink between…*	*Hydrogels disks cut with…*
Protocol 1	2%	2%	0.02%	Manual shaking	Two Petri dishes	Metallic cutter
Protocol 2			0.2%		Two glass plates separated with 2 mm spacers	
Protocol 3				Interconnected syringes		

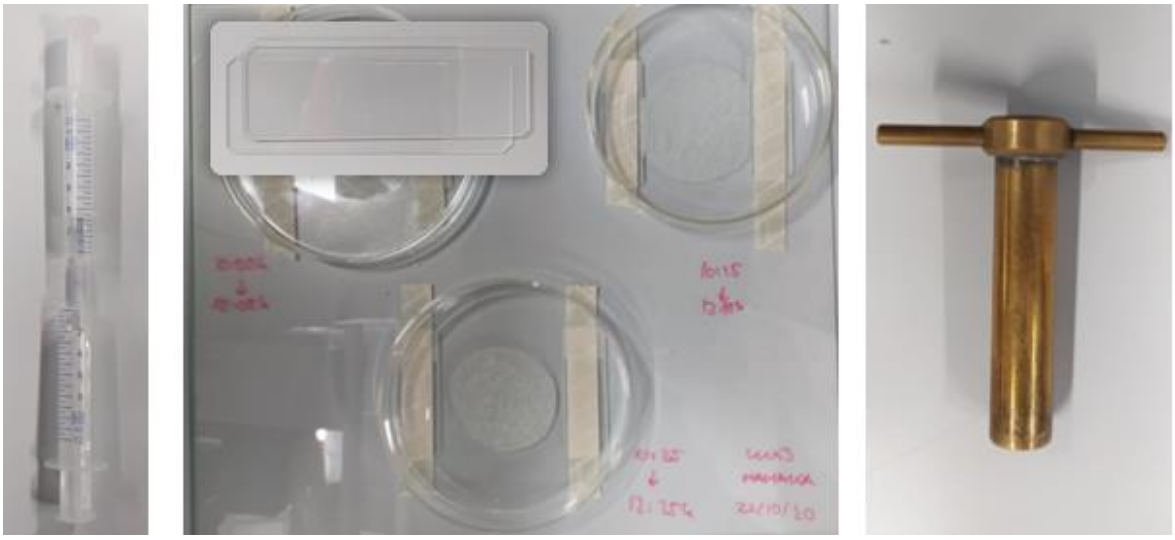

Figure 11: From left to right: Interconnected syringes used for the mixing; Glass plates and spacers; Metallic cutter used to obtain hydrogel disks.

3.2.3. Washing and sterilization

The hydrogels were washed to remove any excess and agglomeration of calcium sulfate. Calcium sulfate in excess may affect physicochemical properties of the hydrogels and it also could cause cells to die. The washing process was optimized throughout the project.

First, the use of water or PBS or both was tried to wash the hydrogels. Table 4 below shows the different washing processes that were tested in this first trial. For the protocol 3 (final protocol), hydrogels were left in distilled water under gentle agitation for at least 24 hours following the crosslinking. During the first hours, water was changed every 15 to 30 minutes.

The hydrogels intended for a use with cells were sterilized with ethanol for 30 to 60 min after the water washing. They were then thoroughly washed with sterilized water to eliminate all the ethanol.

Table 4: Washing processes tested

1st washing	Sterilization	2nd washing	During 3 days
H2O 6x10 min	EtOH 30 min	H2O 6x10 min	X
		PBS 6x10 min	X
		H2O 6x10 min	H2O 3 days
		PBS 6x10 min	PBS 3 days
Final washing process			
In distilled water under gentle agitation for at least 24 hours following the crosslinking. During the first hours, water was changed every 15 to 30 minutes.			

3.3. Alginate functionalization (prior to crosslinking)

To overcome its poor cellular affinity, alginate was functionalized with RGD peptides. To add the peptides, the alginate was modified beforehand with either norbornene or PDEA through Michael additions. The first step of the functionalization was to prepare a 1% (w/v) sodium alginate solution by dissolving alginate in MES buffer (0.1 MES sodium salt, 0.3 NaCl, pH 6.5). The pH of the MES buffer was previously adjusted with 0.1M HCl solution.

3.3.1. Modification with norbornene

The modification with norbornene was based on the protocol described in Ooi et al. [49] with some modifications. EDC was added to the 1% (w/v) alginate solution in needed amount to theoretically activate 5, 20 or 50% of the alginate carboxylic groups. It is important to remark that the real quantity of carboxylic groups activated cannot be known with certainty as the alginate used does not specify the amount of G and M blocks present in the backbone. The pH of the solution has to be very well controlled, as EDC is most reactive in acidic pH [48]. Here, the pH of the MES buffer was 6.5. This was followed by the addition of NHS in a molar ratio 1:2 to EDC. The solution was stirred for 15 min before using pH paper to adjust its pH to approximately 8 with 1M NaOH. Afterwards, norbornene was added in the molar ratio 2:1 to EDC and the reaction was left to stir overnight to ensure modification of the carboxylic groups with norbornene. Afterwards, the solution was dialyzed for 4 days in distilled water

before lyophilization of the product. The membrane used had a pore size of 3500 Da. Molecules with a lower molecular weight present inside the modified alginate pass through the membrane into the water to balance out the difference of concentration. This process is known as osmosis. This specific size of the membrane was chosen as it prevents the alginate from leaving the membrane. Dialysis water was changed every two hours during the first 12 hours and then5-6 times per day. The modified alginate with norbornene will be referred to in the following sections as "alg-Xnorb", X representing the % of carboxyl groups modified (5,20 or 50%).

To modify the alg-norb with the peptide, a 2% (w/v) alg-norb solution in distilled water and a stock solution of LAP (photo initiator) 100mM were prepared. Alginate was left stirring overnight to ensure a complete dissolution. A stock solution of peptides (1mg peptide/mL dH_2O) and a stock solution of LAP at 100mM were prepared. Then, LAP and peptides were added to the alginate solution. 1 mg of peptides was introduced per g of alginate. 47.5 µL, 189 µL or 475µL of LAP were added to modify respectively 5,20 or 50% of the carboxylic groups. The mixture was stirred for 5 min and transferred to a Petri dish to obtain a thin layer of alginate. It was then placed in a customized chamber with a UV lamp (380 nm) and it was incubated for 10 min to allow functionalization of alg-norb with the RGD peptide. It is referred to as alg-Xnorb-1mgRGD.

3.3.2. Modification with PDEA

The modification with PDEA was based on the protocol described in Bubenikova et al. [46]. EDC was added to the 1% (w/v) alginate solution in needed amount to activate 10% of the alginate carboxylic groups. This was followed by the addition of NHS in a molar ratio 1:2 to EDC. The solution was stirred for 15 min before using pH paper to adjust its pH to approximately 8 with 1M NaOH. Afterwards, PDEA was added in the molar ratio 1:1 to EDC and the reaction was left to stir overnight. The reaction solution was dialyzed (membrane size: 3.5kDa) with distilled for 24 hours in water before lyophilization (alg-10PDEA).

Afterwards, a 0.5% (w/v) alg-PDEA solution was obtained by dissolving alg-PDEA in MES buffer. After dissolution, the alginate solution was degassed with N_2 for a few hours in a round-bottom flask. RGD or RGD-CF peptides were dissolved in 1 mL MES buffer, and the equivalent of 1 mg peptides/g alginate was injected into the alginate solution. The mixture was left to react for 24 hours in N_2 atmosphere. The product was dialyzed (membrane size: 3.5kDa) with distilled water for 24 hours before freeze-drying. The product is referred to as alg-10PDEA-1mgRGD.

Fluorescent peptides (RGD-CF) were used to quantify the amount of peptide actually incorporated into the alginate at the end of the reaction.

3.4. Physicochemical characterization

3.4.1. Hydrogels characterization

Scanning Electron Microscopy (SEM)

Scanning electron microscopy (SEM) is a characterization technique to analyze the topography, the morphology, the chemical composition and the crystallinity of a material. To acquire an image, an electron beam is shot onto the surface of the sample and the interactions of the electrons with the surface are measured. The electron beam is composed of primary electrons. When they hit the surface of the sample, different signals are produced, including secondary electrons (SE) and backscattered electrons (BSE). SE originate from the surface of the sample, while BSE come from deeper in the sample. Therefore, SE and BSE provide different information about the material. BSE images are sensitive to differences in atomic number which means they show contrast according to the chemical composition, while SE images give more detailed information on the surface and topography [52].

To study the surface and internal structure of the hydrogels, a scanning electron microscope (Phenom XL Desktop SEM, Quorum Technologies Ltd., UK) was used.

The alginate hydrogels are not conductive and need to be prepared in order to be observed with the SEM. The parts to observe were cut prior to lyophilization to avoid damaging the structure of the hydrogels. After lyophilization, they were pasted on a metallic support. A colloidal solution containing silver was applied in a thin strip to the side and the top of the sample to allow conduction from the metal to the sample. A graphite coating (with graphite rods Grade 1 from Ted Pella) was applied through sputtering on the samples for electron conduction (see Figure 12).

The samples were observed with a pressure of 1 Pa (high vacuum) and a voltage of 10 kV (high resolution). Pictures were taken with a secondary electron detector (SED) and a backscattered electron detector (BSD).

Figure 12: Hydrogel samples after graphite sputtering.

Rheological behavior

Rheology is the study of the deformation and flow of matter under the effect of applied stress. Unlike for Newtonian fluids, the viscosity of non-Newtonian fluids changes with the strain rate. Two main types of behaviors are observed: shear-thinning and shear-thickening. Shear-thinning materials will see a decrease of their viscosity when they are submitted to increased strain rates. On the other hand, the viscosity of shear-thickening materials will increase together with the strain rate.

Rheological tests were carried on 14mm-diameter hydrogel disks with a rheometer (DiscoveryRH-2, TA Instruments, USA, see Figure 13). The optimal testing parameters were determined through preliminary tests. Prewashed hydrogels were left in water for 12 hours prior to the tests. Flow sweep, frequency sweep or axial compression tests were then conducted on the samples. Rough plates were used to prevent wall slip. For hydrogels obtained with Protocol 3, the gap was set to 2300 µm.

The storage (G') and loss (G'') modulus of the hydrogels were measured with a frequency sweep test. The storage modulus is the elastic solid -like behavior, while the loss modulus is the viscous response. The frequency was varied from 0.01 to 10 Hz at 25°C and a constant shear of 1% was applied throughout the whole experiment.

The variations of the hydrogels' viscosity as a function of the shear rate were studied via a flow sweep. The samples were submitted to a shear rate sweep from 1 to 200 s^{-1} at 25°C.

Finally, the axial compression test was performed by applying a compression rate of 5 µm/s during 450 to 660 s at 25°C.

Figure 13: Rheometer.

Swelling behavior

Swelling is an intrinsic property of hydrogels. They expand due to the penetration of water or solvent in the polymeric network.

The swelling behavior of the hydrogels was studied by immersing lyophilized disks in distilled water for several hours. Prior to the test, the dried weight (Wd) of the lyophilized samples was measured. After immersion in water, discs were weighted every 2.5 min. At each time point, hydrogels were wiped on paper before being weighted (Ww). Then they were put back into water. The water was changed every 10 min, contributing to the washing of the hydrogels.

The swelling ratio (SW) was obtained as the ratio between the wet mass of the hydrogel at a time t and the dry mass of the freeze-dried hydrogel: $SW\ (t) = \frac{M_w(t) - M_d}{M_d}$.

Pore size

The pore size was measured with the image-processing software ImageJ. The size of five pores for three different samples was measured. The average of these 15 values was chosen as the average pore size.

Degradation

To test the stability of the hydrogels, they were left in culture medium for 3 days. After 3 days, they were washed and lyophilizated. The surface and the inside of the hydrogels were observed with the SEM.

Weight homogeneity

For each protocol, the weight homogeneity of the hydrogels was measured by weighting five lyophilized samples of different batches.

3.4.2. Modified alginate characterization

Rheological behavior

Rheological tests were also performed on the hydrogels with alg-10PDEA-1mgRGD (HG alg-10PDEA-1mgRGD) to check if they had the same behavior as hydrogels made with normal alginate. The same tests with the same parameters were repeated: flow sweep (shear rate from 1 to 200 s^{-1} at 25°C), frequency sweep (from 0.01 to 10 Hz at 1% strain and 25°C) and axial compression (compression rate of 5 µm/s during 520 s at 25°C).

Fluorescence quantification

A fluorescence test was performed on the alg-10PDEA functionalized with RGD-CF peptide to determine the quantity of peptides incorporated.

The first step was to perform a calibration curve in order to correlate fluorescence values with a particular concentration. To do so, RGD-CF was dissolved in distilled water to prepare solutions of decreasing peptide concentration. Ten solutions with concentrations ranging from 10 µM to 0 nM were prepared. 50 µL of each concentration of the standard curve were added to a 96-well plate with black bottom and fluorescence intensity was read (λexcitation = 485 nm, λemission = 528 nm) using a microplate reader (In- finite M200 PRO, Tecan Group Ltd., Männedorf, Switzerland), thus obtaining a calibration curve matching every peptide concentration with a fluorescence value.

Then, 50 µL of the 2% non-modified alginate and of the alginate containing RGD-CF were also prepared and their fluorescence was measured.

Fourier Transformation Infrared (FTIR) spectroscopy

FTIR spectroscopy is a method used to study the chemical structure and composition of organic and inorganic compounds. A multichromatic source of IR radiation goes through a series of mirrors (the interferometer) to the sample, which partly absorbs the radiation. The radiation not absorbed by the sample is then detected to obtain an infrared spectrum of the transmittance versus the wave numbers (which is proportional to the frequency). Each type of molecular bonds absorbs at a particular frequency, thus conferring at each molecule a unique infrared spectrum. Two methods can be used in FTIR spectroscopy: transmission or attenuated total reflection (ATR). In transmission technique, the IR light passes directly through the sample. In ATR technique, the IR light passes through a crystal in contact with the sample. The crystal is most often made of germanium, diamond or zinc selenide [53], [54]. The instrumentation of an IR spectrometer is shown in Figure 14.

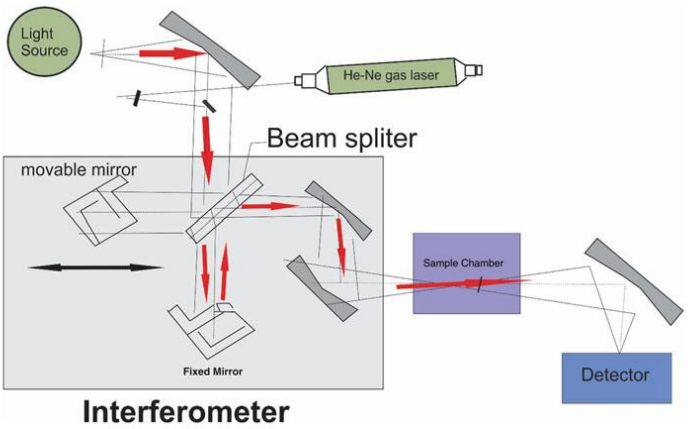

Figure 14: Instrumentation of the FTIR spectrometer [54].

FTIR spectroscopy was performed on normal alginate and modified alginate to check that the alginate had indeed been modified. The spectra were recorded on a FTIR spectrometer (Nicolet 6700) in transmission mode, between 400 and 4000 cm^{-1}. The ATR method with a germanium crystal cannot be used on alginate, as alginate and germanium absorb at the same frequency.

To prepare the samples, alginate powder and lyophilizated modified alginates reduced to powders were used. The powders were mixed with bromide potassium KBr with 1:10 ratio and grinded finely. Afterwards, they were pressed into a fine disk.

The spectra were recorded and processed with the software OMNIC.

4. Results and discussion

4.1. Optimization of the fabrication process of hydrogels

4.1.1. Influence of the hydrogel composition

Crosslinker: $CaCl_2$ vs. $CaSO_4$

The use of $CaCl_2$ as a crosslinker was rejected: the shape and the homogeneity of the hydrogels were hard to control due to the fast and uncontrolled cross-linking. The gelation with $CaSO_4$ was slower, allowing more time for the mixing before the alginate was totally crosslinked. This is due to the lower solubility of $CaSO_4$ in water: the release of Ca^{2+} ions takes longer and slows down the gelation.

Crosslinker concentration

The best results in terms of consistency were achieved with $CaSO_4$ in a final concentration in the hydrogels of 2% (w/v) (60mM). For lower concentrations (10,20,40 and 50 mM), the hydrogels were too soft, and for higher concentrations (100,120 and 500 mM), they were too stiff. The rigidity of the hydrogels increases with the concentration of calcium ions because the crosslinking is more extensive.

The concentration of the $CaSO_4$ stock solution impacted the homogeneity of the hydrogel. A concentration of 1.22M allowed a better mixing than 3M because the volume injected was more important and less concentrated.

Alginate concentration

The concentration of alginate was also an important factor. The best results in terms of consistency were obtained for a concentration of 2% (w/v). Initially, alginate solutions of 3 and 4% (w/v) were prepared, however, they were too viscous to be easily used. Hydrogels made with solutions of concentration below 2% were not consistent enough and did not retain their shape well.

The effects of the composition on the characteristics of the hydrogels are summed up in Table 5.

$(NaPO_3)_6$ concentration

Different concentrations (0.02%, 0.2%, 1% and 2%) of the retarding agent $(NaPO_3)_6$ were tested. By slowing down the crosslinking of the hydrogel, it eases the fabrication process. The mixture can be manipulated for a longer time before gelation, allowing better mixing and shaping. A concentration of **0.2% (w/v) of $(NaPO_3)_6$** was found to be the best compromise between the homogeneity of the hydrogel and its crosslinking time. For low concentrations of retarding agent, the crosslinking was too

fast. The hydrogels were already crosslinking during the mixing process. Thus, it was not possible to give the hydrogels the desired shape. While higher concentrations of $(NaPO_3)_6$ resulted in better homogeneity, the crosslinking time was too long to be practical (more than 2 hours).

It is also probable that the composition and purity of the alginate used impact greatly the crosslinking time. For similar concentration of phosphate-based agent, the crosslinking time of our hydrogel was much longer than what is reported in the literature [26]. This is probably due to the lesser quality of G-blocks in our alginate.

Table 5: Influence of the composition on the hydrogels.

	Concentration		
	<2%	**2%**	>2%
Alginate	Hydrogels not consistent enough	Good	Alginate too viscous to be used
$CaSO_4$	Hydrogels are too soft	Good	Hydrogels are too stiff
$CaCl_2$	The shape and homogeneity of the hydrogel is not controlled enough		
	Concentration		
	<0.2%	**0.2%**	>0.2%
$(NaPO_3)_6$	Crosslinking too fast to get a good shape and mixing	Good	Crosslinking too slow, not practical

4.1.2. Washing and sterilization

After crosslinking, agglomerates and residues of calcium sulfate were visible at the surface and inside the hydrogels. It is important to remove the calcium sulfate that did not participate in the crosslinking through a washing process, as it could influence the mechanical properties of the hydrogels and be toxic for the cells.

H_2O vs. PBS

The difference was clear between the samples left three days in PBS and the samples left three days in water. The samples washed in PBS broke easily, especially on the edges. On the other hand, the consistency of the samples washed in water did not change even after three days; and they were easier

to manipulate compared to the PBS-washed samples. For this reason, only water was used for the final washing process.

Figure 15: Lyophilizated hydrogels washed with PBS (left) and water (right).

Efficiency and impact of washing and sterilization

A first observation with the naked eye suggested that the washing process with water was efficient in removing the excess calcium sulfate. A more detailed observation was then carried out with SEM. The images obtained are presented in Figure 16.

Images of unwashed hydrogels (Figure 16a) showed important quantities of calcium sulfate, trapped inside the hydrogel and on its surface. After washing (Figure 16b), the hydrogel was much cleaner, with little to no trace excess of calcium sulfate. The more the hydrogel was washed, the cleaner it was. Moreover, washing the hydrogel with distilled water did not cause any change in its internal structure.

In one case, a mass uptake of a lyophilizated hydrogel was observed after the washing process. This was not logical: after removal of the excess of calcium sulfate, the hydrogel should be lighter than it was before washing it. The observation of that sample with SEM revealed the presence of bacteria (see Figure 17). This was observed only on one sample and it is probably because the washing was not carried out on sterile conditions and it was neither changed regularly, so there was a contamination of the hydrogel with bacteria.

To avoid the contamination with bacteria, samples for cellular use were sterilized 30 minutes with ethanol after the first washing (Figure 16c). After sterilization samples were washed with distilled water for at least 2 hours, changing water every 20 minutes to ensure a total removal of ethanol. SEM images showed that the sterilization did not impact the structure of the hydrogel and prevented the contamination of the hydrogels with bacteria (see Figure 16c).

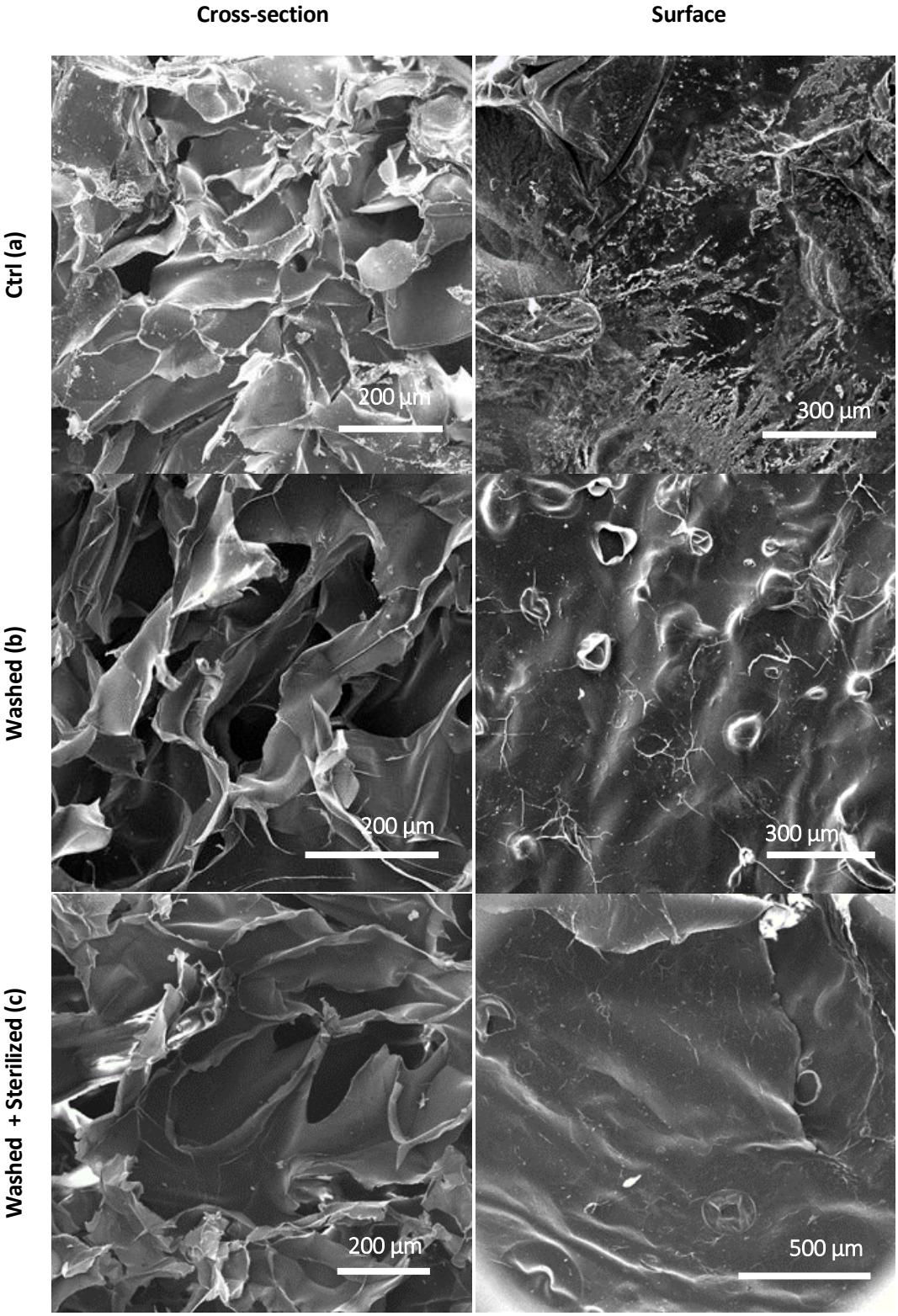

Figure 16: Effect of the washing (b) and sterilization (c) on the cross-section (I) and surface (II) of hydrogels. SEM images obtained with SED.

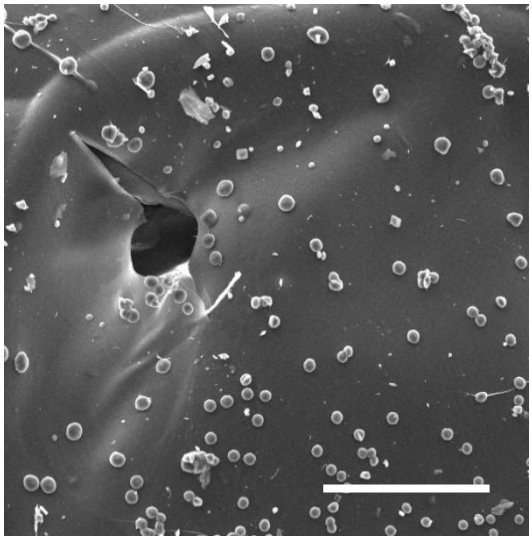

Figure 17: Proliferation of bacteria on washed hydrogel. SEM image (scale bar = 50 µm).

4.1.3. Homogeneity and reproducibility

The fabrication protocol of the hydrogels was improved throughout the project. The idea was to increase the homogeneity:

→ In terms of shape, composition and physicochemical properties

Homogeneity within a batch and between batches is crucial to get reproducible results with a specific protocol. Every time a protocol is reproduced, the hydrogels disks obtained should be the most similar possible in terms of shape, composition and properties.

→ In terms of distribution of the crosslinker in the hydrogel

Having a good mixing and dispersion of the calcium sulfate is important for the homogeneity of the properties within a sample. In particular, calcium sulfate agglomerates (see Figure 18) should be avoided.

Figure 18: Agglomerates of calcium sulfate in a hydrogel.

To ensure homogeneity of the hydrogels, the next parameters were measured:

- Mass of the hydrogels
- Formation of air bubbles
- Rheological properties

Comparison between the 3 protocols

For the **protocol 1**, the mixing was done by shaking the mixture manually in a tube. It was hard to obtain a good compromise between the shaking time and the quality of the mixing. Usually, the mixture had already started to crosslink in the tube before the alginate and the calcium sulfate had mixed correctly, because shaking is not a very efficient way of mixing. As the mixture slowly start to gel, it gets more viscous, which means it gets even more difficult for the calcium sulfate to spread evenly. If the mixture had already started to crosslink by the time it was put between two Petri dishes, the hydrogels obtained were friable and broke easily. Since some parts had already started crosslinking, it was also harder to get a flat surface. Finally, there was nothing to control the thickness from one batch to another.

For the **protocol 2**, two glass plates separated with spacers were used instead of the Petri dishes. It allowed a better control of the thickness and helped smooth the surface.

Finally, for the **protocol 3**, the mixing was improved. The pressure applied to the interconnected syringes improves the dispersion of the calcium sulfate solution and its even distribution in the alginate.

The Table 6 below sums up the differences of the protocols.

Table 6 : Comparison of the protocols

	Mixing by..	**Left to crosslink between...**
Protocol 1	Manual shaking	Two Petri dishes
Protocol 2		Two glass plates separated with spacers
Protocol 3	Interconnected syringes	

Better mixing

Constant thickness and smooth surface

Mass variation associated with each protocol

After washing and lyophilization, the hydrogels were weighted. The mean dried mass of hydrogels and the standard deviation for each of the three fabrication processes are shown in Figure 19.

The improvement of the hydrogels' fabrication process is associated with a decrease in the standard deviation of the hydrogels' dried masses. Protocol 1 has the higher standard deviation, whereas protocol 3 has the smallest one. We can assume that the smaller the standard deviation of a protocol is, the more homogeneous mass the hydrogels have between themselves. Their shape and their composition are more likely to be similar. For example, hydrogels disks cut from a batch with uneven thickness or containing agglomerates of calcium sulfate will have a higher standard deviation of the mean mass.

The decrease in dried mass observed every time the protocol was improved is explained by a more controlled and lower thickness and by a better washing. For protocol 1, the thickness of the hydrogels was not controlled and was usually at least 3mm. For protocol 2, the thickness was 3mm while for protocol 3, the thickness was 2mm. Moreover, the washing process was constantly improved throughout the project so samples from protocol 3 were the cleanest. The removal of calcium sulfate in excess contributes to the mass decrease.

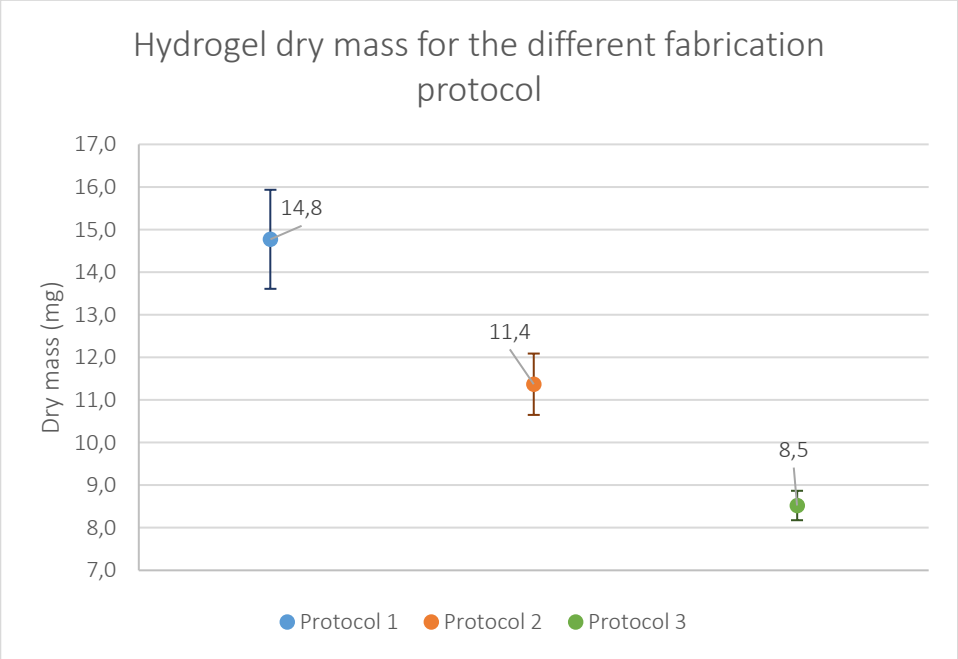

Figure 19: Mean mass and standard deviation of the hydrogels (9 samples) for each protocol.

Air bubbles

The removal of air in the alginate solution and in the pipette during the fabrication process of hydrogels is also very important. The presence of air causes the formation of air bubbles in the hydrogels as seen in Figure 20. The rehydration of hydrogels following lyophilization also created air bubbles inside the hydrogels, although the exact reason is not known. The same phenomenon was observed when the hydrogels were frozen and unfrozen: as they melted, bubbles appeared. Several methods (centrifugation, sonication, temperature) were tried to get rid of the bubbles but none of them succeeded. These air bubbles can impact the homogeneity of the hydrogels' properties which is why it is important to avoid their formation.

To avoid these bubbles, the solution was to use the hydrogels directly after their production. In this case, there were not any air bubbles.

Figure 20: Presence of air bubbles in a hydrogel.

Homogeneity of rheological properties

The relative standard deviation of the storage modulus and loss modulus for each protocol is shown on Table 7. The data was obtained with a frequency sweep. The relative standard deviation was calculated as: $standard\ deviation\ of\ the\ modulus/mean\ modulus$. It indicates whether the data is tightly clustered around the mean or not.

Table 7: Mean values and relative standard deviation of the storage modulus and loss modulus

	Protocol 1	Protocol 2	Protocol 3	
			Batch 1	Batch 2
Mean storage modulus (Pa)	608.4	2319.8	1684.7	1893.3
Mean standard deviation of the storage modulus (Pa)	44.2	448.1	499.8	575.4
Relative standard deviation of the storage modulus (Pa)	7.2 %	19 %	29.7 %	30.2 %
Mean loss modulus	45.5	281.3	202.3	276.71
Mean standard deviation of the loss modulus	3.6	59.2	51.0	85.2
Relative standard deviation of the loss modulus	7.9 %	21 %	25.2 %	30.8 %

An increase in the relative standard deviation of each modulus is seen for each protocol. It shows that although the homogeneity in terms of shape and mass was improved for each new protocol, the homogeneity in the rheological properties of the hydrogels has decreased.

However, it is important to note that for the first protocols, the hydrogels that did not seem homogeneous (presence of calcium sulfate agglomerates, uneven shapes…) were discarded and were not used for the rheological tests. As the fabrication process improved, the hydrogels made seemed visually more acceptable (no agglomeration of calcium sulfate, no bubbles…) and most of them were kept for the rheological tests. So although the relative standard deviation is smaller for the earliest protocols, it is not necessarily representative of the homogeneity of the protocol.

4.2. Characterization of the hydrogels

4.2.1. Internal structure and porosity

An example of a SEM image of the internal structure of the hydrogels obtained using protocol 3 is displayed in Figure 21a. A porous three-dimensional structure is seen, similar to what can be observed in the literature [26] (see Figure 21b). The pores are oval and well defined, with a diameter of about **250 µm x 112 µm** (see Figure 22b). A pore size between 200 and 400 µm is considered as optimal for bone regeneration [5]. Pore size is crucial to get appropriate cell infiltration and vascularization. High porosity improves the diffusion of nutrients within the hydrogel network. Furthermore, it is also possible to see the interconnectivity of pores (see Figure 22a), also important to facilitate vascularization and cell infiltration.

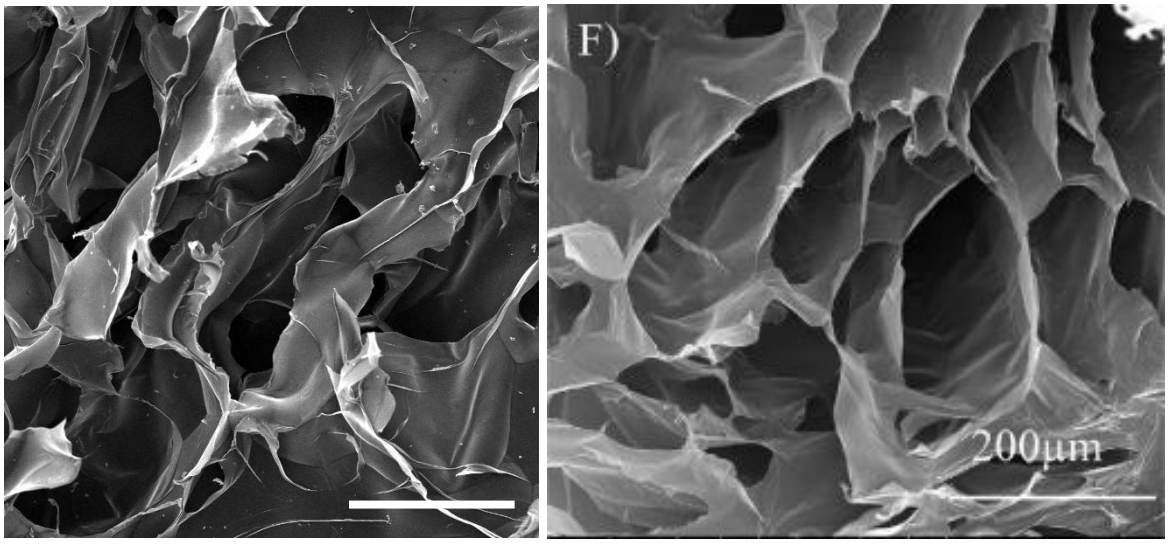

a) b)

Figure 21: Alginate hydrogel internal microstructure from a) Protocol 3 (scale bar=200µm) and b) Espona et al. [26]. SEM images obtained with SED.

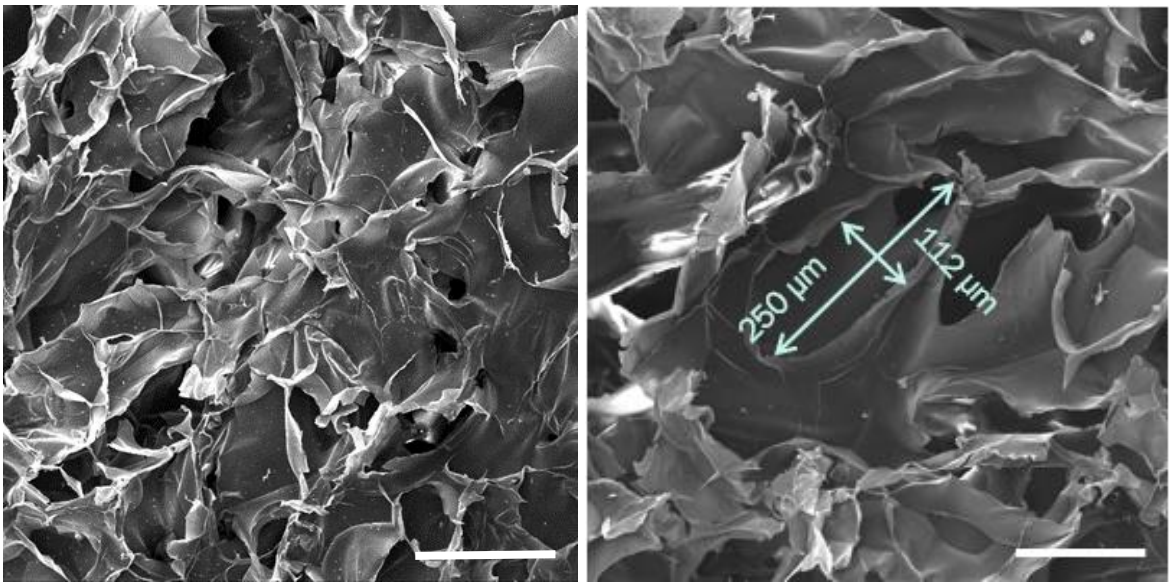

a) b)

Figure 22: a) Interconnectivity of pores (scale bar = 300 µm) and b) pore size in a hydrogel (scale bar = 200 µm). Hydrogels fabricated with protocol 3. SEM images with SED.

4.2.2. Rheological behavior

Flow sweep

The evolution of the viscosity as a function of the shear rate was obtained from the flow sweep test (see Figure 24). The alginate hydrogels exhibited a **shear-thinning** behavior, which means the viscosity decreases when the shear rate increases. When a shear stress is applied to an entangled network, the molecular chains stretch and untangle until they are completely aligned (see Figure 23). The more aligned the chains of the polymers are, the easier it flows, which means it is less viscous. When the shear rate increases, the hydrogel shows more resistance to the shear, which translates into higher stress values.

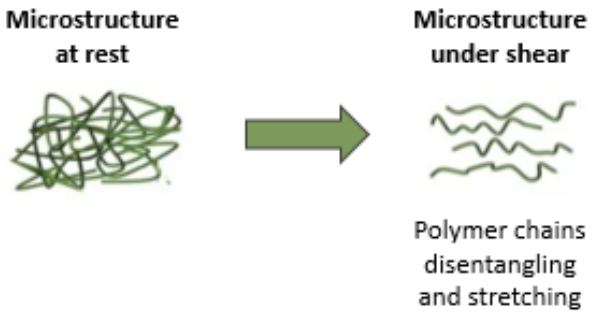

Figure 23: Response of polymer chains to shear [55].

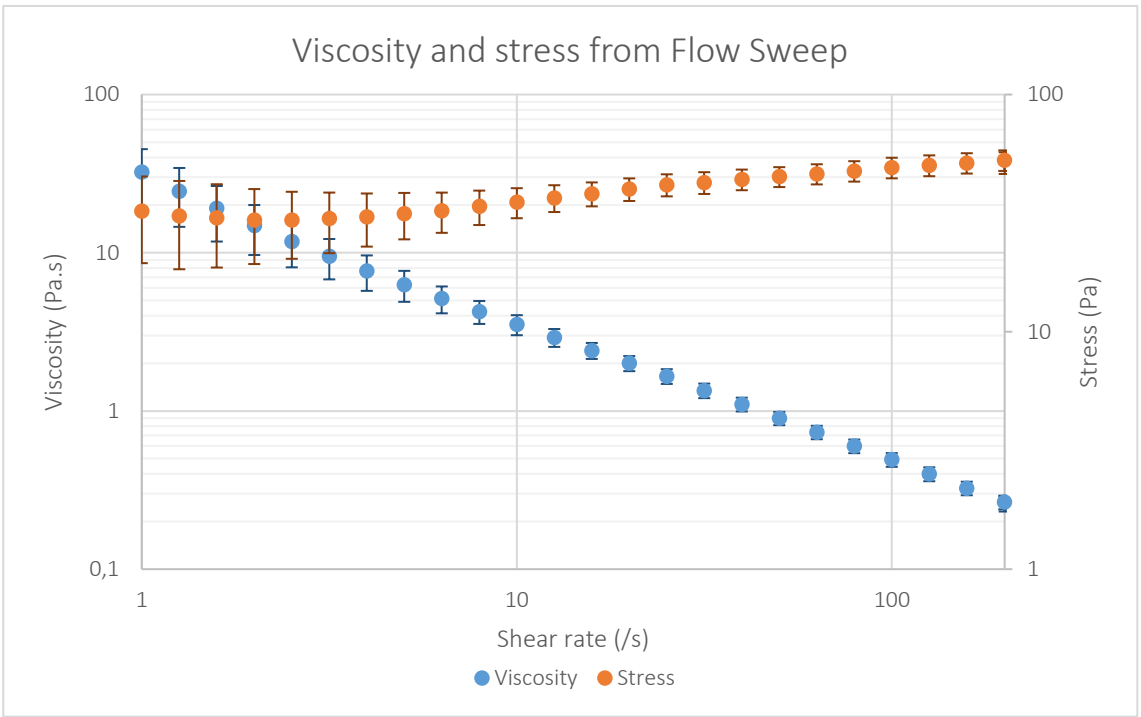

Figure 24: Viscosity and stress evolution obtained from a flow sweep with shear rates from 1 to 200 s-1, 1% strain and at 25°C. Performed on 5 hydrogels synthetized with protocol 3.

Frequency sweep

The frequency sweep gave information about the evolution of the storage and loss modulus over a frequency range.

The storage modulus is much higher than the loss modulus (about seven times higher) (see Figure 25). The storage modulus represents the ability of the hydrogel to store deformation energy and to return to its initial configuration before a mechanical force was applied. A storage modulus higher than the loss modulus shows that the elastic component is dominant over the viscous component. This relates to the extent of the crosslinking: the more crosslinked the hydrogel is, the higher its storage modulus will be, and it will have more the characteristics of a solid rather than those of a liquid (see Figure 26).

Overall, the values of storage and loss modulus can be considered as constant over the frequency range. This indicates a stable crosslinking, and that the hydrogel maintains its structure during the experiment.

A slight increase of the storage modulus associated to a slight decrease of the loss modulus is observed throughout the frequency sweep. During the test, the hydrogel is pressed between the top and bottom plates of the rheometer. Some water is squeezed out of the hydrogel, especially at higher frequencies since the oscillation rate is faster. By losing some of the water it was retaining, the hydrogel loses a bit of its “liquid” component, which results in a lower loss modulus and a higher storage modulus.

Similar results in terms of tendencies (constant modulus over frequency range, G’>>G”) are observed in the literature. The values vary a lot depending on the precise composition of the hydrogels and the conditions and parameters of the tests.

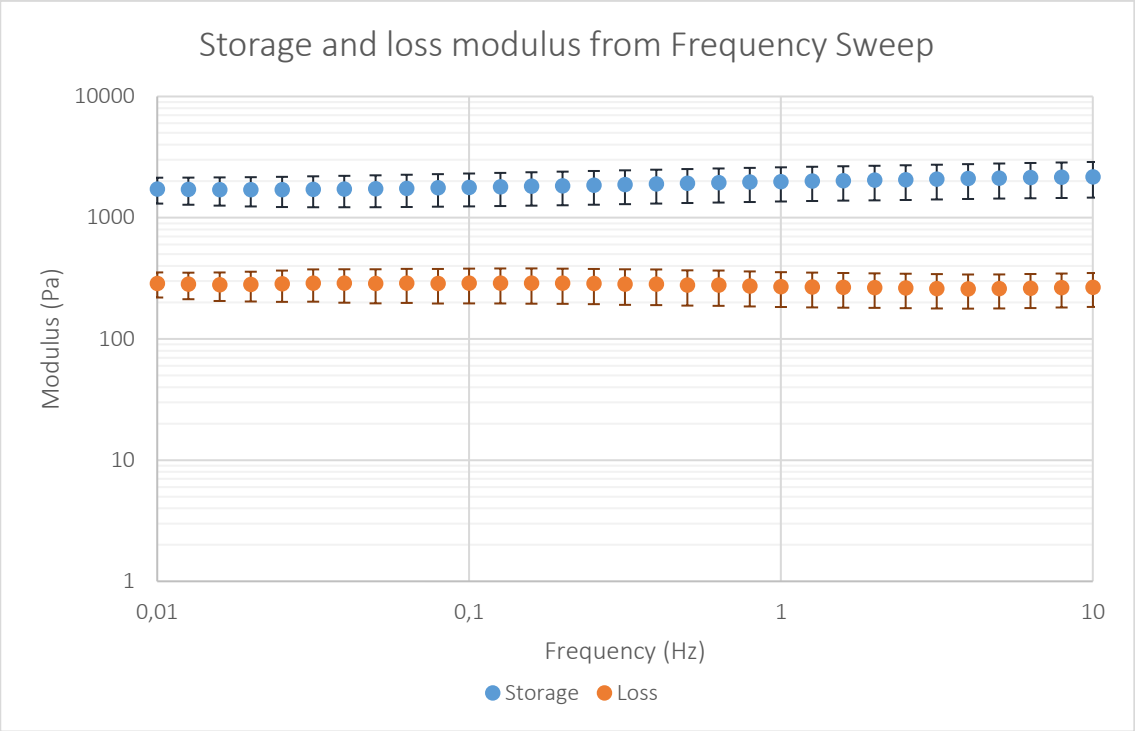

Figure 25: Storage and loss modulus from a frequency sweep between 0.01 and 10 Hz at 25°C. Performed on 5 hydrogels synthesized with protocol 3.

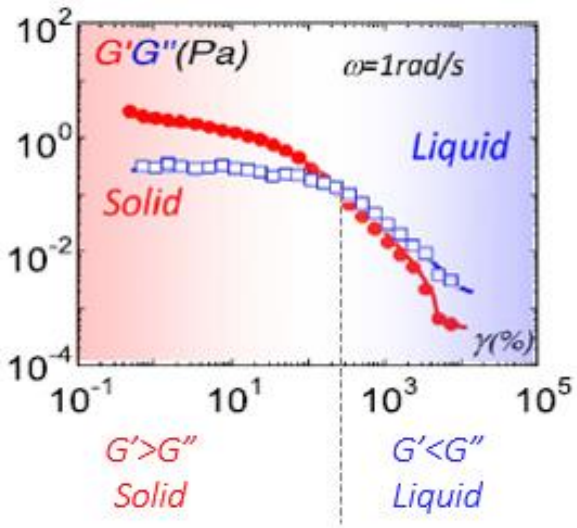

Figure 26: Evolution of storage and loss modulus for a solid and a liquid [56].

Axial compression

Under the influence of an axial compression, the hydrogel showed a high strain rate (up to 80% of its initial thickness) before network failure as put in evidence on Figure 27. If the test is stopped before failure, the hydrogel quickly regains its initial thickness following rehydration. This testifies to its elastic behavior and can be linked with the storage modulus.

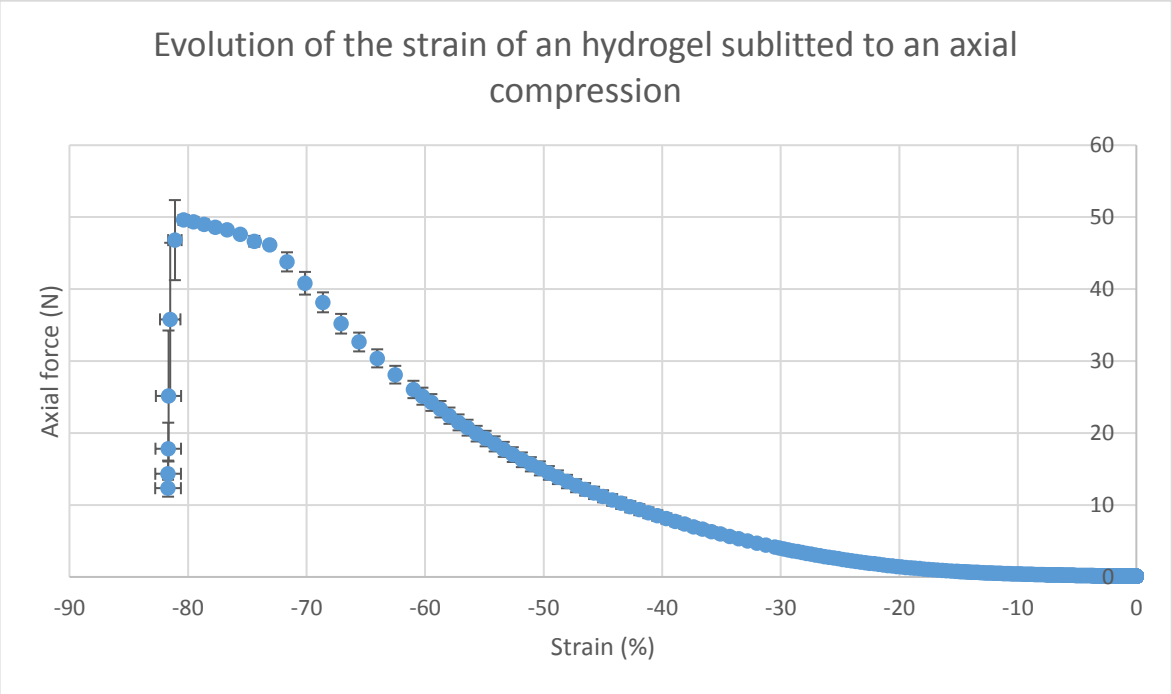

Figure 27: Axial force vs. strain from an axial compression with a compression rate of 5 µm/s at 25°C. Performed on hydrogels synthetized with protocol 3.

4.2.3. Swelling behavior

The evolution of the swelling ratio over time is presented in Figure 28. The swelling ratio increases quickly, before reaching a plateau after about 45 min. The plateau value is around 50, which means the hydrogel absorbed 50 times its dry weight in water. This demonstrates the highly absorbent nature of hydrogels. In the literature, swelling ratios around 30 were usually obtained [26], [57].

The swelling ratio depends on the degree of crosslinking: a higher swelling ratio means the hydrogel is less crosslinked. When a hydrogel is more crosslinked, the network is tighter, and its swelling is limited.

Overall, the swelling ratio increases until it reaches a plateau. However, experimentally, some decreases can be seen. This might be due to the way of taking the measures. For each measure, the hydrogel is quickly wiped on paper before being weighted. However, the quantity of water absorbed will obviously vary for every measure, which impact the swelling ratio.

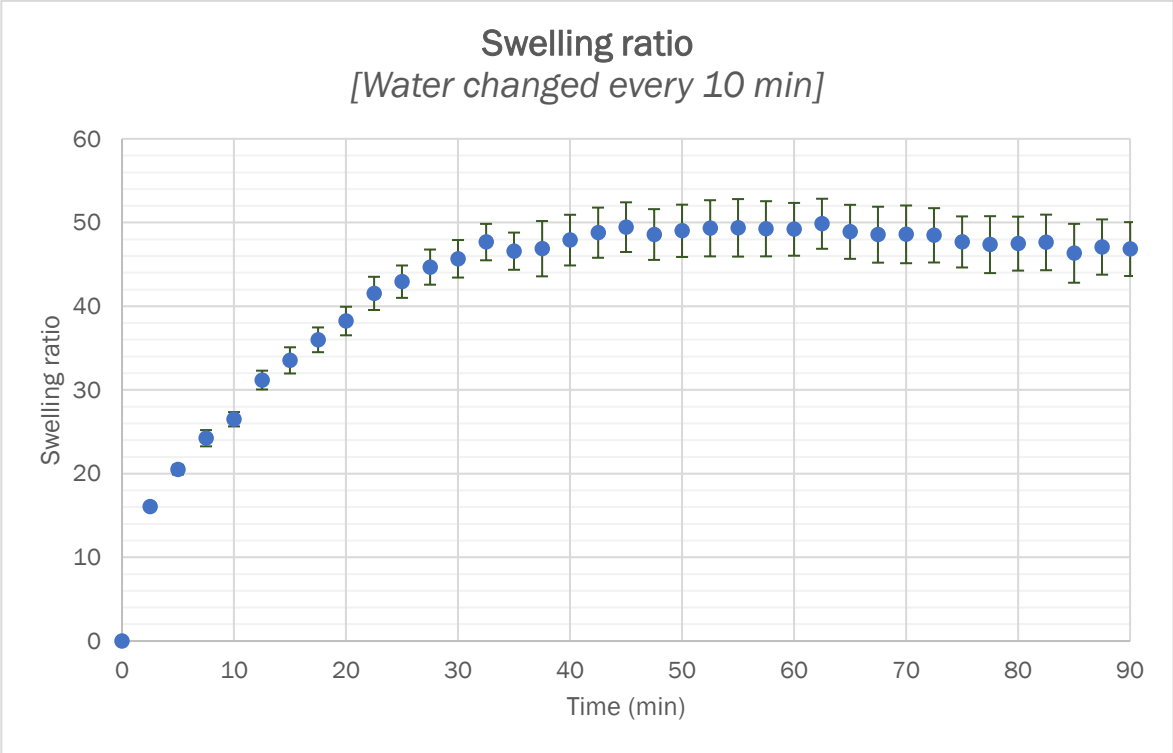

Figure 28: Evolution over time of the swelling ratio of alginate hydrogels. Performed on 5 hydrogels made with protocol 3.

4.2.4. Degradation

After 3 days in culture medium, there was not any visible degradation of the hydrogel. The structure observed with SEM (see Figure 29) seems to be a bit different compared to a hydrogel that was not in culture medium. The pores are more elongated and a bit thinner (400µm x 101µm compared to 250µm x 112µm for normal hydrogels).

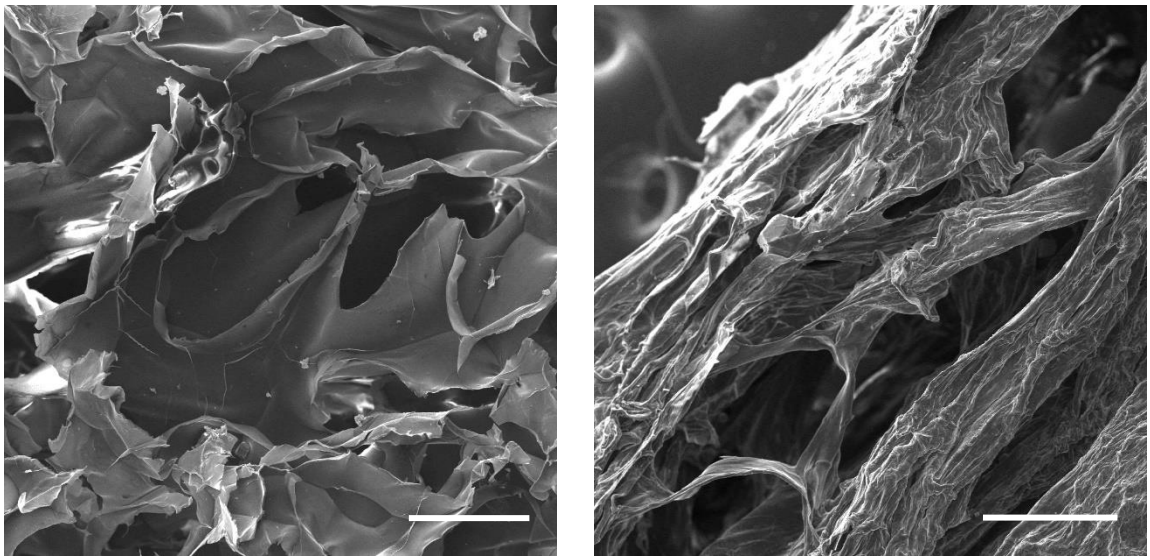

a) b)

Figure 29: Comparison between the structure of a) normal hydrogel (scale bar = 200µm) and b) hydrogel after 3 days in culture medium (scale bar = 200µm). Hydrogels fabricated with protocol 3. SEM images obtained with SED.

4.2.5. Cell adhesion experiments

Biological experiments were carried out by other members in the group. Such studies were performed by adding hMSCs in the hydrogels during their fabrication using protocol 3. The cells were added to the syringe containing alginate and mixed 15 times very gently with the alginate. Then, a live/dead staining test was performed to observe the cell behavior after 1, 4, 7 and 12 days. Calcein 3µM was used to stain the live cells and propidum iodide (PI) 4µm was used to stain the dead cells. The results are shown in Figure 30.

After 1 day, cells were homogeneously distributed on the hydrogel. The cells in green are the live cells, whereas the red cells are dead. They were probably killed by the mechanical action of the mixing during the synthesis of the hydrogels. After 4 days, some dead cells were still visible, meaning that there were still some cells dying to the mixing process. However, after 7 and 12 days, only live cells were observed. The hydrogel is not toxic for the cells and does not kill them: the cells are stable.

The cells on the hydrogel presented a roundish shape. This is normal because bulk alginate lacks cell adhesion points, so cells could not attach to the alginate. Furthermore, cell did not proliferate due to the same reason. However, after 12 days in culture, cells were still alive, which demonstrates the good performance and biocompatibility of the hydrogel.

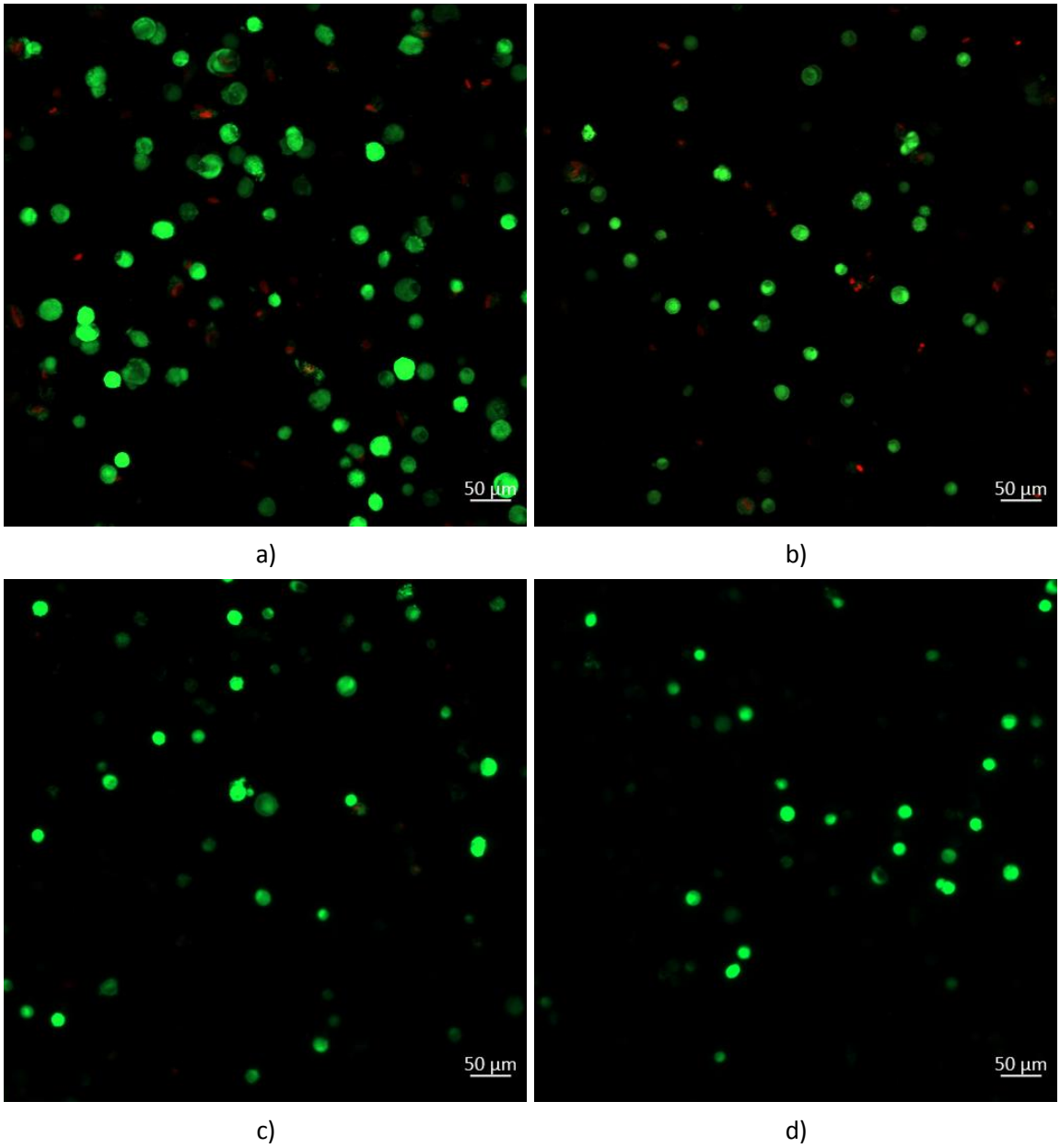

Figure 30: Results from live/dead test on unmodified alginate hydrogels after a) 1 day, b) 4 days, c) 7 days and d) 12 days.

4.3. Characterization of the modified alginate

4.3.1. Rheological behavior

Flow sweep

As shown on Figure 31, the HG alg-10PDEA-1mgRGD have a shear-thinning behavior, like the HG alg. The difference in the values is probably due to the difference in thickness of the hydrogels. Although both types of hydrogels were initially the same thickness, the HG alg-PDEA-1mgRGD swelled more during the washing process, which caused them to be a bit thicker. For all the rheological tests, the gap was set at 2300 µm, which means the HG alg-10PDEA-1mgRGD were more compressed compared to the HG alg. This impacted the stress values and the viscosity measured.

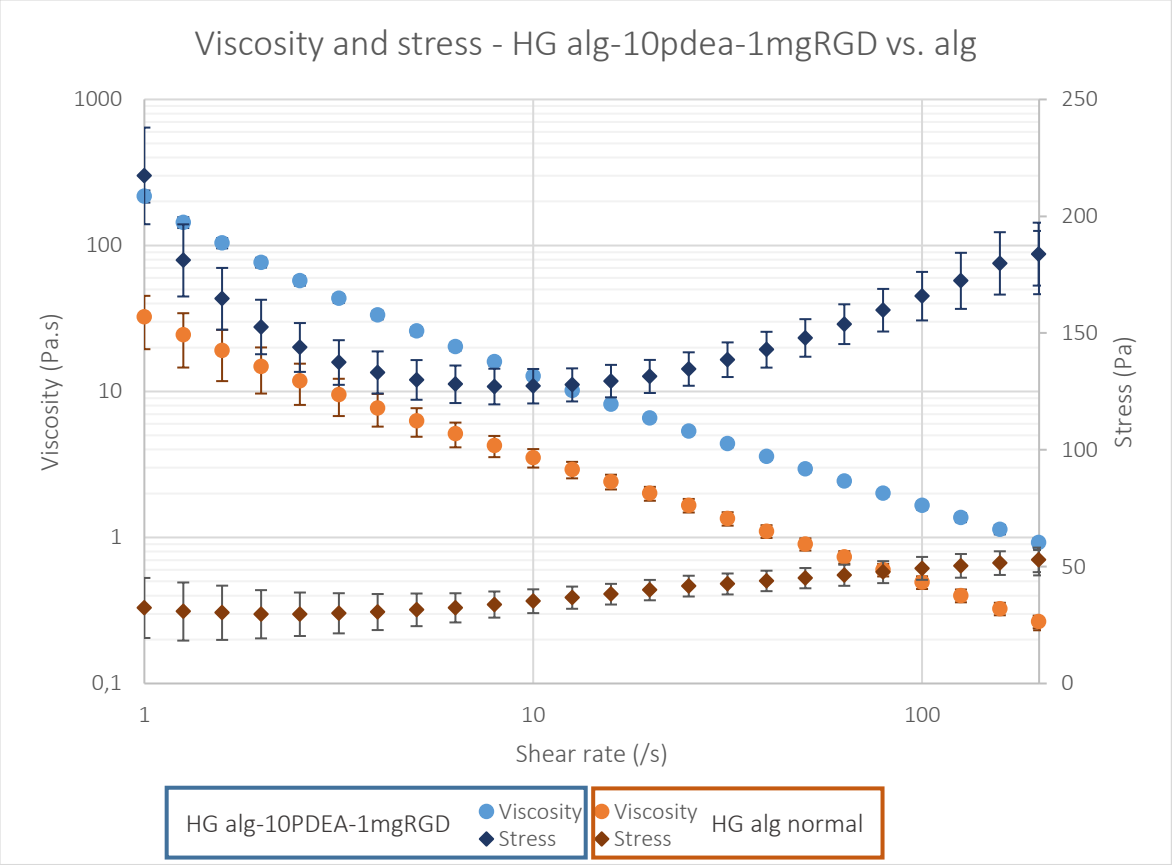

Figure 31: Viscosity and stress comparison between HG alg-10PDEA-1mgRGD vs. HG alg. From a flow sweep with shear rates from 1 to 200 s-1, 1% strain and at 25°C. Performed on 5 hydrogels for each.

Frequency sweep

The results from the frequency sweep performed on the HG alg-10PDEA-1mgRGD were compared with the ones from the HG alg (from protocol 3) and are shown on Figure 32.

The tendencies of the curves are similar between HG alg and HG alg-10PDEA-1mgRGD: in both cases, the storage modulus is higher than the loss modulus and the modulus are overall constant over the range of frequency. For the loss modulus, the values are very similar. For the storage modulus, however, the values of HG-alg-10PDEA-1mg-RGD are twice higher than the values of HG-alg. A higher storage modulus usually indicates a higher extent of crosslinking. However, here, it is not in accordance with the swelling observed during the washing process, which rather suggests a lower crosslinking degree. The difference observed could be due again to the difference of the thickness between the two types of hydrogels. Since the same value of gap was used, more water was squeezed from the HG alg-10PDEA-1mgRGD, that were thicker.

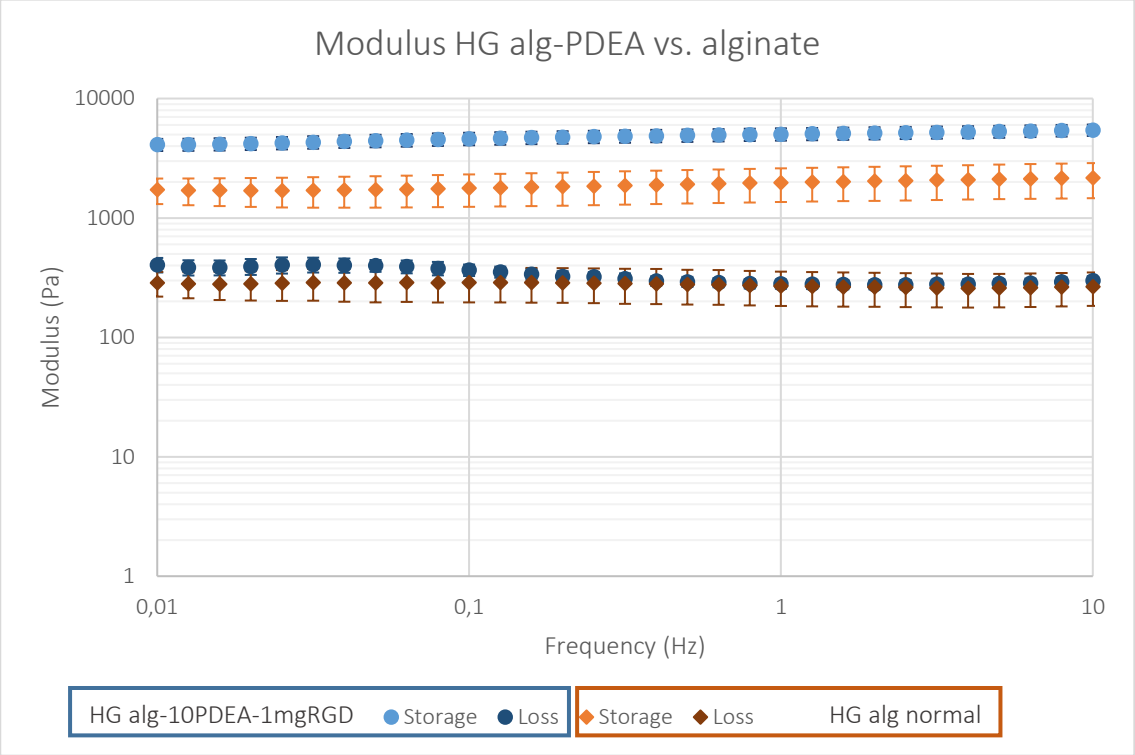

Figure 32: Comparison of the storage and loss modulus between HG alg-10PDEA-1mgRGD and HG alg (protocol 3). From a frequency sweep between 0.01 and 10 Hz at 25°C. Performed on 5 hydrogels for each case.

Axial compression

The functionalized hydrogels are also very elastic. Figure 33 shows that the HG alg-10PDEA-1mgRGD can deform more than the HG alg before failure. This is probably because they are slightly less crosslinked.

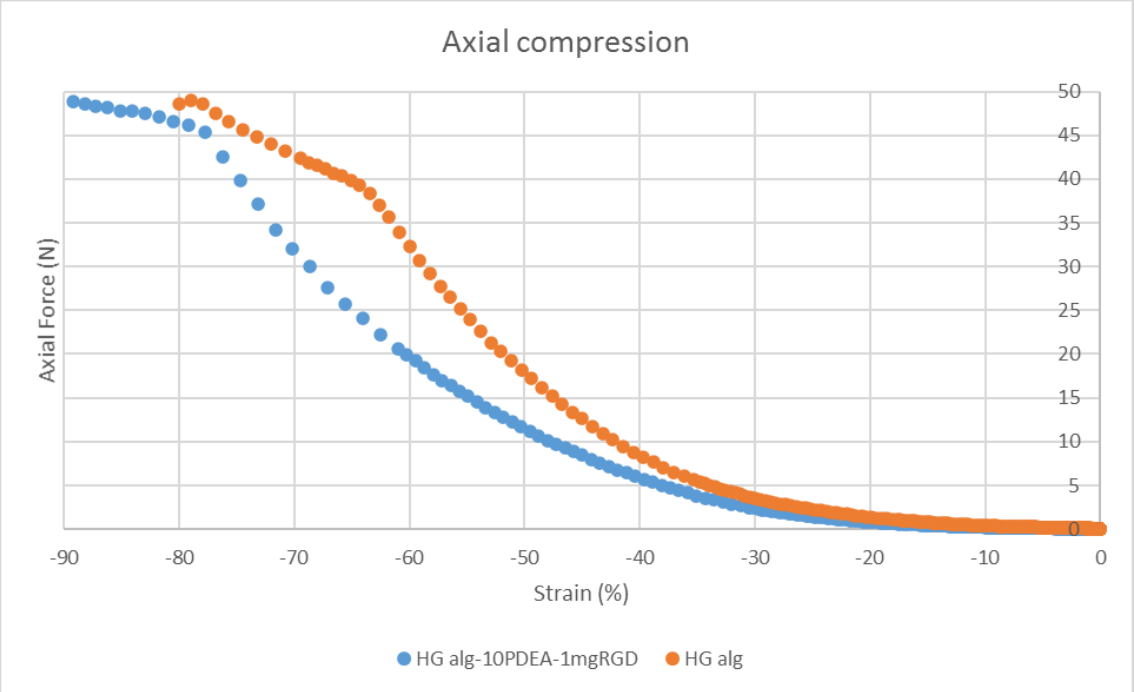

Figure 33: Comparison of the axial force vs. strain between HG alg-10PDEA-1mgRGD and HG alg (protocol 3). From an axial compression with a compression rate of 5 µm/s at 25°C.Performed on 5 hydrogels for each case.

4.3.2. Incorporation of peptides and modification of the alginate

Fluorescence test

The incorporation of RGD peptides in the alg-PDEA-1mgRGD was quantified by modifying the alginate with fluorescent peptides. The fluorescence test data was modelized by a linear function y=ax+b, correlating the fluorescence values to the concentration of peptides. Initially, 1 mg peptide was added per g of alginate. By extrapolation, it was found that **0.76 mg peptide/g alginate** were incorporated in the alginate. This is a very good result as most of the peptides introduced (76%) were incorporated. For example, in Bubenikova's work [46], for a quantity of 1mg peptide/g alginate, the coupling efficiency was only around 40%.

This test was only performed on the alginate modified with PDEA and not on the alginate modified with norbornene due to lack of time.

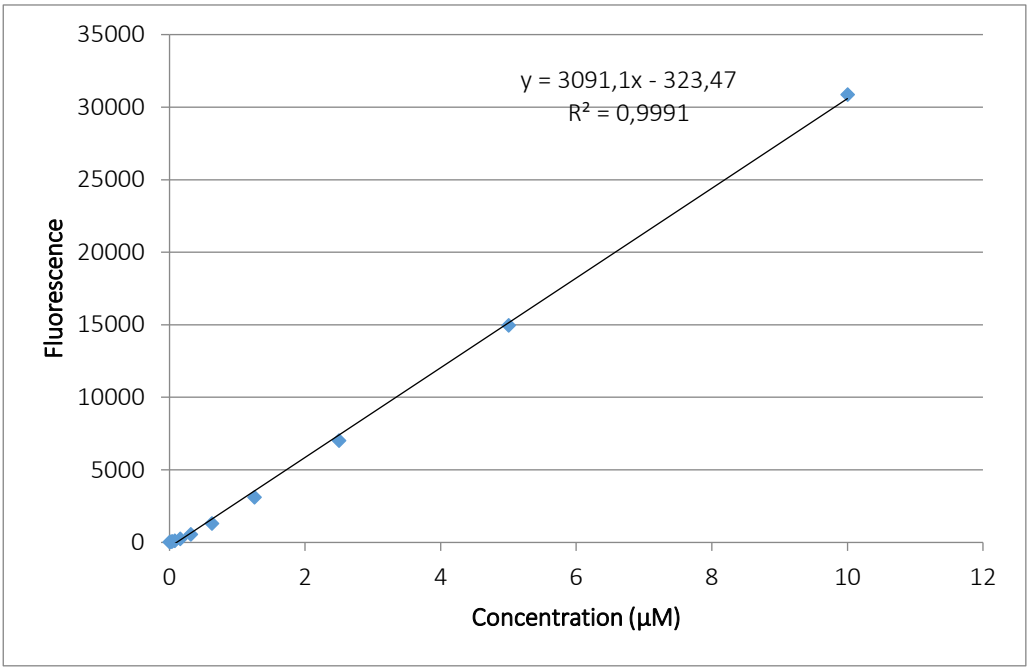

Figure 34: Calibration curve showing the fluorescence as a function of the peptide concentration.

FTIR spectroscopy

FTIR spectroscopy was also performed to analyze the modification of the alginate with norbornene and PDEA and its functionalization with peptides. However, the spectra obtained were difficult to interpret because the results obtained were not as satisfactory as expected and because many of the bonds and functional groups present in the peptides are also present in the rest of the molecule.

The modification with PDEA introduces a disulfide group (see Figure 35). The presence of a disulfide group (S – S bond) should be characterized by a peak between 500 and 700 cm^{-1}. The spectra of alg-10PDEA-1mgRGD presents a very small peak at 675 cm^{-1} which could suggest the presence of PDEA. However, that peak was only barely visible on the alg-10PDEA spectra. (see Figure 36)

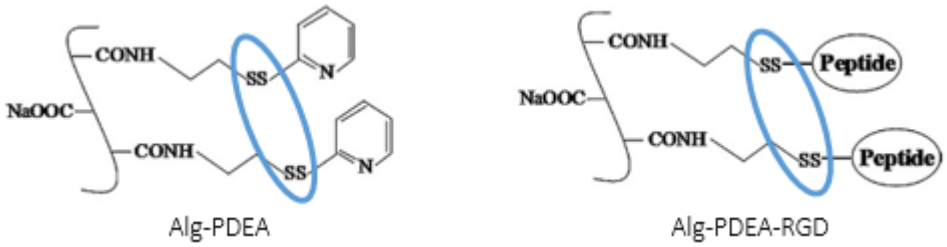

Figure 35: Presence of S – S bonds in alg-PDEA and alg-PDEA-RGD.

The presence of amide groups (C=O stretching) should be associated with a strong peak between 1650 and 1700 cm^{-1}. However, none of the spectra has a peak in that range.

A strong and thin peak is seen on the alg-50norb spectra at 1275 cm^{-1}. This peak is not visible on any of the other spectra: it is not on the alg-20norb (see Figure 37) nor on the alg-50norb-1mgRGD (see Figure 38 and Figure 38).

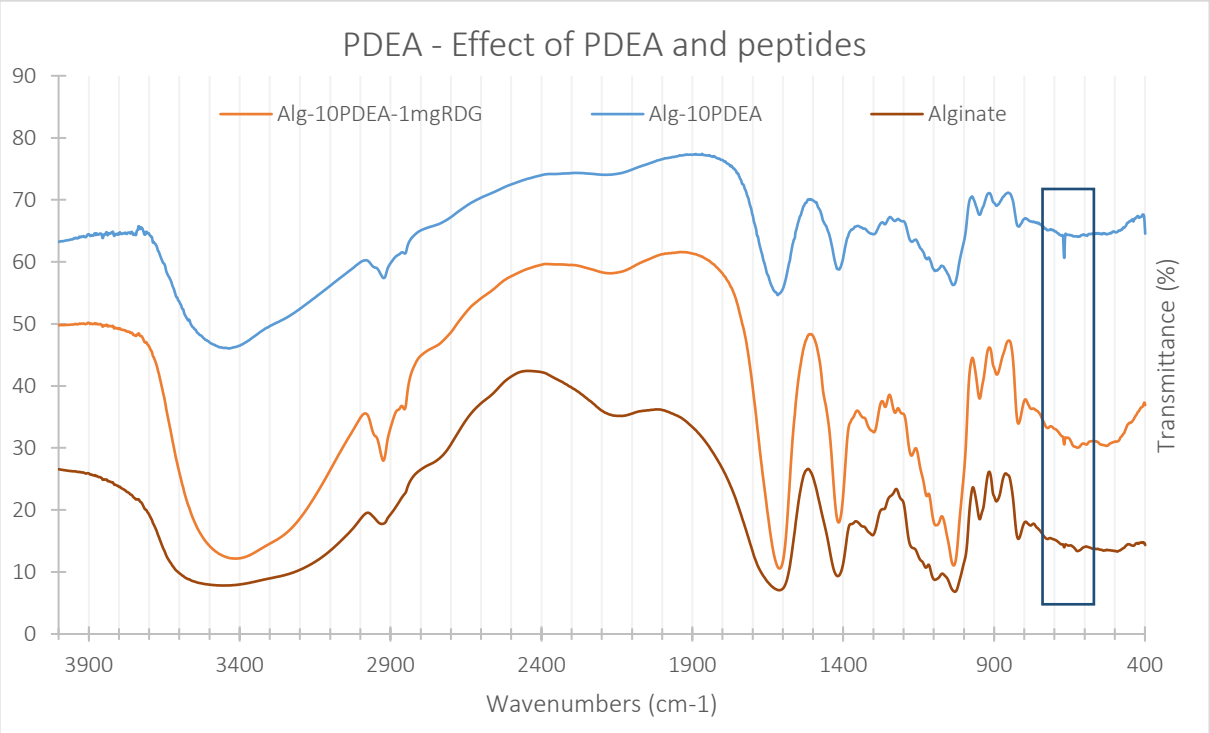

Figure 36: FTIR spectra showing the effect of PDEA and peptides on the alginate.

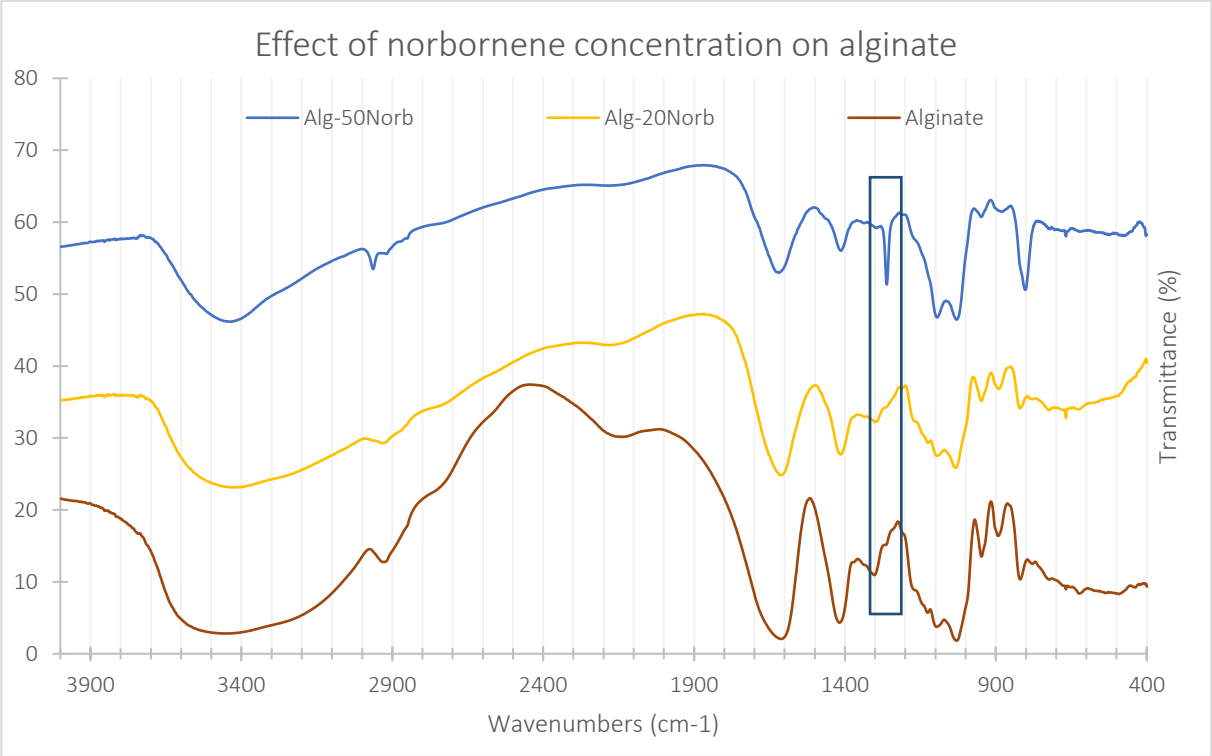

Figure 37: FTIR spectra showing the effect of the norbornene concentration on the alginate.

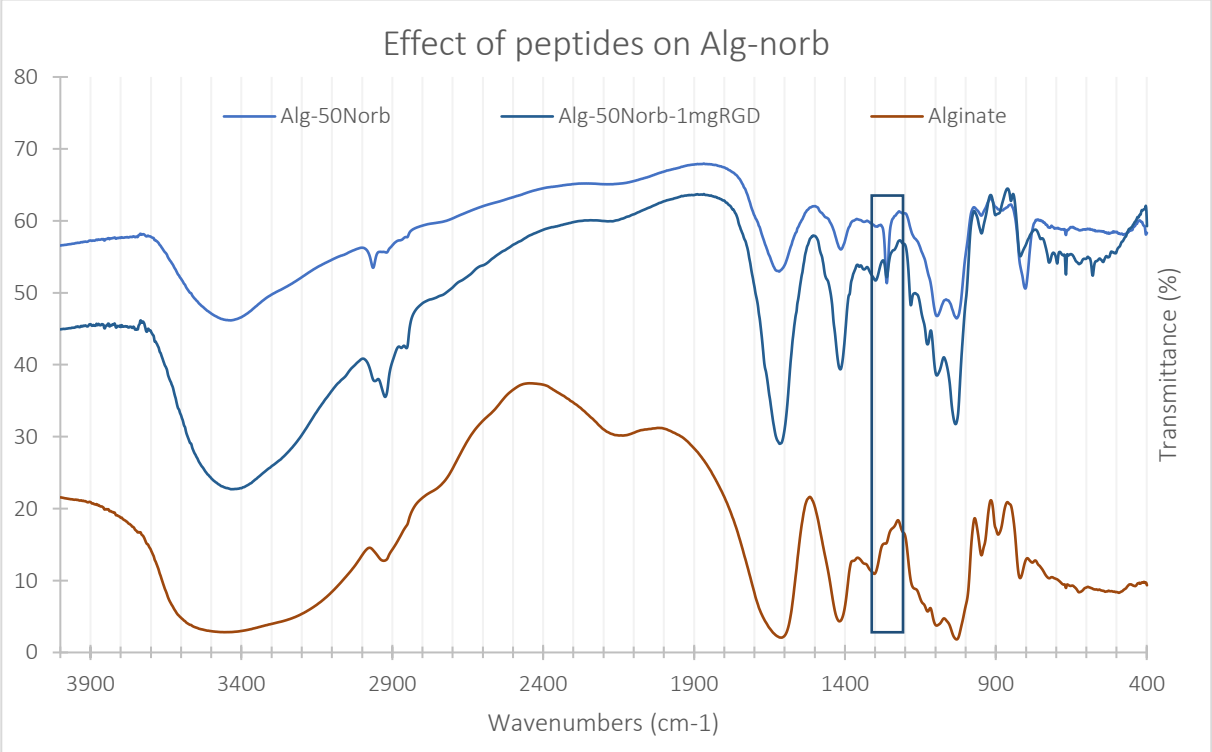

Figure 38: FTIR spectra showing the effect of norbornene and peptides on the alginate.

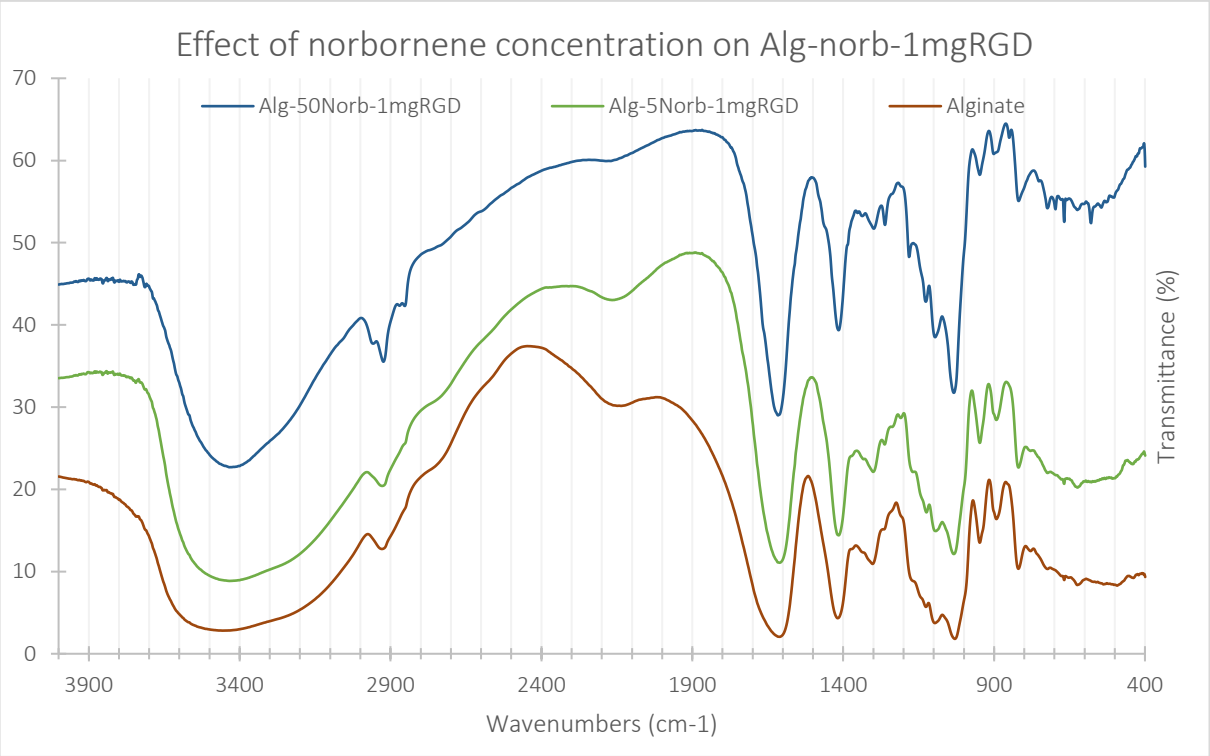

Figure 39: FTIR spectra showing the effect of norbornene concentration on the functionalized alginate.

4.3.3. Cell adhesion experiments

Biological experiments were carried out by other members in the group. Such studies were performed by adding hMSCs on lyophilizated hydrogels made with alg-50norb-1mgRGD (HG alg-50norb-1mgRGD) and on lyophilizated hydrogels made with alg-10PDEA-1mgRGD (HG alg-10PDEA-1mgRGD). After 1 day, a live/dead staining test was performed to observe the cell behavior. Calcein 3µM was used to stain the live cells and propidum iodide (PI) 4µm was used to stain the dead cells.

The test was done to see if the functionalization of the alginate with RGD peptides was successful. It was done on hydrogels modified with norbornene (HG alg-Xnorb-1mgRGD) and on hydrogels modified with PDEA (HG alg-10PDEA-1mgRGD) to compare the two functionalization protocols. For the protocol with norbornene, the test was done only on HG alg-**50**norb-1mgRGD (this is the highest concentration of norbornene tested). This is the condition with the most carboxyl groups modified, so theoretically, all peptides could potentially attach themselves to the alginate. The results are shown in Figure 40.

After one day, stretched cells were observed on both HG alg-50norb-1mgRGD (see Figure 40b) and HG alg-10PDEA-1mgRGD (see Figure 40c). This confirms that the functionalization of the alginate with both methods has been successful. The behavior of cells on non-modified alginate is shown on Figure 40a

for comparison. In this condition, there were less cells attached and the ones that could attach were roundish.

The cells seem more stretched on the HG alg-10PDEA-1mgRGD than on the HG alg-50norb-1mgRGD, suggesting that the functionalization protocol with PDEA might be the best one.

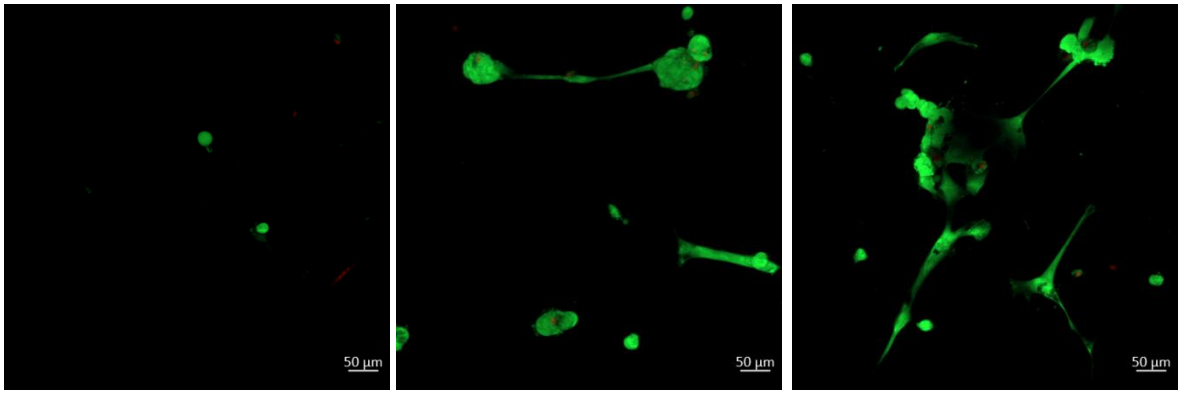

a) b) c)

Figure 40: Live/dead test on a) HG alg, b) HG alg-50norb-1mgRGD and c) HG alg-10PDEA-1mgRGD.

Conclusions

The objectives of this work were to synthetize alginate-based hydrogels, functionalize the alginate and characterize the hydrogels and the functionalized alginate.

The composition and initial protocol to fabricate hydrogels were adapted from previous works. The protocol was then modified and optimized throughout the project to improve the homogeneity of the shape and mass of the hydrogels and to improve the mixing of the calcium sulfate inside the hydrogels. The washing process showed removal of most of the excess calcium sulfate without damaging the structure of the hydrogels. The hydrogels present a porous structure with a pore size around 250 µm and have the typical behavior of a hydrogel, such as shear-thinning, great elasticity and high swelling ratio.

The alginate was functionalized with 1 mg of RGD peptides per g of alginate, through modification with either norbornene or PDEA. Live/dead staining confirmed the successful functionalization of the alg-50norb and alg-10PDEA. The quantity of peptides incorporated in the alg-PDEA was evaluated through fluorescent spectroscopy. A high incorporation rate of 76% was measured. This measure was not done on the alg-norb due to lack of time, however, the results obtained so far are in favor of the functionalization with PDEA. Good results were obtained and the protocol is faster compared to the one with norbornene (the dialysis times are shorter).

Ongoing and future work

Several aspects can be further investigated.

- → Improve the reproducibility of the protocol to get more homogeneous properties from one sample to another.
- → Verify that the alg-norb-RGD has been functionalized with a fluorescence test or by NMR.
- → Characterize further the hydrogels synthesized with alg-PDEA-RGD (SEM, swelling test) and compare their properties to normal hydrogels.
- → Characterize further the hydrogels synthesized with alg-norb-RGD (rheology, SEM, swelling test) and compare their properties to normal hydrogels.
- → Conclude on the functionalization protocol that works best.
- → Functionalize the alginate with higher quantities of peptides.
- → Functionalize the hydrogels after crosslinking.

Analysis of the environmental impact

The environmental impact was taken into account throughout this project. The use of single-use material (pipette tips, well-plates, plastic recipients…) was avoided when possible. Non-contaminated plastic recipients were washed and re-used several times.

The water contaminated during the dialysis of norbornene-modified alginate was thrown away in the container for non-halogenated solvents. The pipette tips and plastic pipettes used to manipulate products containing norbornene were thrown in the contaminated solid waste container.

Budget

Three types of cost are associated to the project: the ones relative to materials, the ones relative to the equipment and the ones relative to the staff. They are presented in the tables below.

Table 8: Cost of the materials used in the project.

MATERIALS			
	Quantity	Price	Cost (€)
24-well plate	20	65€/5 plates	260
Falcon 50 mL	30	150€/500 units	9
Falcon 15 mL	7	200€/500 units	2,8
Gloves S size	80	5€/boxes	80
Tips 1 mL	100	54.17€/960 units	5,6
Tips 200 µL	100	59.28€/960 units	6,2
Tips 5 mL	5	66.17€/960 units	0,3
Alginate	15 g	1€/kg	0,015
Calcium sulfate hemihydrate	177g x 35	25.70€/500 g	318,4
Distilled water	150	0.1€/L	15
Pasteur pipette 3 mL	7	23.30€/500 units	0,3
Total cost for equipment			697,6

Table 9: Cost of the staff involved in the project.

PERSONAL			
	Worked hours (h)	Salary (€/h)	Cost (€)
Master student	650	0	0
PhD student	100	42	4200
Project director	15	60	900
Technical team	10	32.97	329.7
Total cost for staff			5429,7

Table 10: Cost of the equipment used in the project.

EQUIPMENT			
	Time of use (h)	Price (€/h)	Cost (€)
SEM	18	40	720
Rheometer	25	40	1000
Lyophilizator	450	5	2250
FTIR	10	40	400
Microplate reader	0.2	40	8
Total cost for equipment			4378

Table 11: Total cost of the project;

Cost total of the project	
	Cost (€)
Staff	5429,7
Equipment	4378
Material	697,6
TOTAL	10505,3€

Bibliography

[1] X. Lin, S. Patil, Y. G. Gao, and A. Qian, "The Bone Extracellular Matrix in Bone Formation and Regeneration," *Frontiers in Pharmacology*, vol. 11, no. May. pp. 1–15, 2020, doi: 10.3389/fphar.2020.00757.

[2] X. Bai, M. Gao, S. Syed, J. Zhuang, X. Xu, and X. Q. Zhang, "Bioactive hydrogels for bone regeneration," *Bioact. Mater.*, vol. 3, no. 4, pp. 401–417, 2018, doi: 10.1016/j.bioactmat.2018.05.006.

[3] "Anatomy & Physiology Portal | Britannica." https://www.britannica.com/browse/Anatomy-Physiology (accessed Nov. 25, 2020).

[4] N. Rucci, "Molecular biology of bone remodelling," *Clinical Cases in Mineral and Bone Metabolism*, vol. 5, no. 1. pp. 49–56, 2008.

[5] H. D. N. Tran, K. D. Park, Y. C. Ching, C. Huynh, and D. H. Nguyen, "A comprehensive review on polymeric hydrogel and its composite: Matrices of choice for bone and cartilage tissue engineering," *J. Ind. Eng. Chem.*, vol. 89, pp. 58–82, 2020, doi: 10.1016/j.jiec.2020.06.017.

[6] R. Dimitriou, E. Jones, D. McGonagle, and P. V Giannoudis, "Bone regeneration: Current concepts and future directions," *BMC Medicine*, vol. 9. 2011, doi: 10.1186/1741-7015-9-66.

[7] J. Block and L. E. Miller, "Perspectives on the clinical utility of allografts for bone regeneration within osseous defects: a narrative review," *Orthop. Res. Rev.*, no. April, p. 31, 2011, doi: 10.2147/orr.s18397.

[8] T. Albrektsson and C. Johansson, "Osteoinduction, osteoconduction and osseointegration," *Eur. Spine J.*, vol. 10, pp. S96–S101, 2001, doi: 10.1007/s005860100282.

[9] S. Durual, "L'ostéointégration," *BioMatériaux Clin.*, vol. 2, pp. 72–75, 2017.

[10] F. Mahyudin, D. N. Utomo, H. Suroto, T. W. Martanto, M. Edward, and I. L. Gaol, "Comparative Effectiveness of Bone Grafting Using Xenograft Freeze-Dried Cortical Bovine, Allograft Freeze-Dried Cortical New Zealand White Rabbit, Xenograft Hydroxyapatite Bovine, and Xenograft Demineralized Bone Matrix Bovine in Bone Defect of Femoral Di," *Int. J. Biomater.*, vol. 2017, 2017, doi: 10.1155/2017/7571523.

[11] R. Yoshida, S. Baron, C. Rodner, and J. Ferreira, "Biologics in hand surgery," in *Biologics in Orthopaedic Surgery*, Elsevier, 2018, pp. 135–139.

[12] M. C. Mendoza, B. D. Rosenthal, and W. K. Hsu, "Biologic Options in Interbody Fusion," in *Lumbar Interbody Fusions*, Elsevier, 2019, pp. 145–149.

[13] N. J. Hickok, C. Ketonis, and C. S. Adams, "Tethered antibiotics," in *Comprehensive Biomaterials*, vol. 4, Elsevier, 2011, pp. 281–294.

[14] A. E. Rodriguez and H. Nowzari, "The long-term risks and complications of bovine-derived xenografts: A case series," *J. Indian Soc. Periodontol.*, vol. 23, no. 5, pp. 487–492, Sep. 2019, doi: 10.4103/jisp.jisp_656_18.

[15] H. J. Haugen, S. P. Lyngstadaas, F. Rossi, and G. Perale, "Bone grafts: which is the ideal biomaterial?," *J. Clin. Periodontol.*, vol. 46, no. S21, pp. 92–102, 2019, doi: 10.1111/jcpe.13058.

[16] P. V. Giannoudis, H. Dinopoulos, and E. Tsiridis, "Bone substitutes: an update.," *Injury*, vol. 36 Suppl 3, pp. 20–27, 2005, doi: 10.1016/j.injury.2005.07.029.

[17] H. H. K. Xu *et al.*, "Calcium phosphate cements for bone engineering and their biological properties," *Bone Res.*, vol. 5, no. August, pp. 1–19, 2017, doi: 10.1038/boneres.2017.56.

[18] M. P. Ginebra, M. Espanol, Y. Maazouz, V. Bergez, and D. Pastorino, "Bioceramics and bone healing," *EFORT Open Rev.*, vol. 3, no. 5, pp. 173–183, 2018, doi: 10.1302/2058-5241.3.170056.

[19] M. Navarro, A. Michiardi, O. Castaño, and J. A. Planell, "Biomaterials in orthopaedics," *J. R. Soc. Interface*, vol. 5, no. 27, pp. 1137–1158, 2008, doi: 10.1098/rsif.2008.0151.

[20] D. L. Millis, "Responses of Musculoskeletal Tissues to Disuse and Remobilization," in *Canine Rehabilitation and Physical Therapy: Second Edition*, 2013.

[21] A. Arifin, A. B. Sulong, N. Muhamad, J. Syarif, and M. I. Ramli, "Material processing of hydroxyapatite and titanium alloy (HA/Ti) composite as implant materials using powder metallurgy: A review," *Mater. Des.*, vol. 55, no. January 2018, pp. 165–175, 2014, doi: 10.1016/j.matdes.2013.09.045.

[22] N. Shayesteh Moghaddam *et al.*, "Metals for bone implants: safety, design, and efficacy," *Biomanufacturing Rev.*, vol. 1, no. 1, pp. 1–16, 2016, doi: 10.1007/s40898-016-0001-2.

[23] C. Shi, Z. Yuan, F. Han, C. Zhu, and B. Li, "Polymeric biomaterials for bone regeneration," *Ann. Jt.*, 2016, doi: 10.21037/aoj.2016.11.02.

[24] S. J. Buwalda, K. W. M. Boere, P. J. Dijkstra, J. Feijen, T. Vermonden, and W. E. Hennink, "Hydrogels in a historical perspective: From simple networks to smart materials," *J. Control. Release*, vol. 190, pp. 254–273, 2014, doi: 10.1016/j.jconrel.2014.03.052.

[25] A. C. Hernández-González, L. Téllez-Jurado, and L. M. Rodríguez-Lorenzo, "Alginate hydrogels for bone tissue engineering, from injectables to bioprinting: A review," *Carbohydr. Polym.*, vol. 229, no. May 2019, p. 115514, 2020, doi: 10.1016/j.carbpol.2019.115514.

[26] A. Espona-Noguera *et al.*, "Tunable injectable alginate-based hydrogel for cell therapy in Type 1 Diabetes Mellitus," *Int. J. Biol. Macromol.*, vol. 107, no. PartA, pp. 1261–1269, 2018, doi: 10.1016/j.ijbiomac.2017.09.103.

[27] D. P. Bhattarai, L. E. Aguilar, C. H. Park, and C. S. Kim, "A review on properties of natural and synthetic based electrospun fibrous materials for bone tissue engineering," *Membranes (Basel).*, vol. 8, no. 3, 2018, doi: 10.3390/membranes8030062.

[28] R. Donate, M. Monzón, and M. E. Alemán-Domínguez, "Additive manufacturing of PLA-based scaffolds intended for bone regeneration and strategies to improve their biological properties," *E-Polymers*, vol. 20, no. 1. De Gruyter Open Ltd, pp. 571–599, Jan. 01, 2020, doi: 10.1515/epoly-2020-0046.

[29] X. Bi and A. Liang, "In Situ-Forming Cross-linking Hydrogel Systems: Chemistry and Biomedical Applications," in *Emerging Concepts in Analysis and Applications of Hydrogels*, 2016.

[30] G. Thakur, F. C. Rodrigues, and K. Singh, "Crosslinking Biopolymers for Advanced Drug Delivery and Tissue Engineering Applications," in *Advances in Experimental Medicine and Biology*, 2018.

[31] M. Liu *et al.*, "Injectable hydrogels for cartilage and bone tissue engineering," *Bone Res.*, vol. 5, no. November 2016, 2017, doi: 10.1038/boneres.2017.14.

[32] X. Li, Q. Sun, Q. Li, N. Kawazoe, and G. Chen, "Functional hydrogels with tunable structures and properties for tissue engineering applications," *Frontiers in Chemistry*. 2018, doi: 10.3389/fchem.2018.00499.

[33] J. Xu, Y. Liu, and S. hui Hsu, "Hydrogels based on schiff base linkages for biomedical applications," *Molecules*, vol. 24, no. 16, pp. 1–21, 2019, doi: 10.3390/molecules24163005.

[34] K. T. Nguyen and J. L. West, "Photopolymerizable hydrogels for tissue engineering applications," *Biomaterials*, vol. 23, no. 22, pp. 4307–4314, 2002, doi: 10.1016/S0142-9612(02)00175-8.

[35] T. N. Vo, F. K. Kasper, and A. G. Mikos, "Strategies for controlled delivery of growth factors and cells for bone regeneration," *Advanced Drug Delivery Reviews*, vol. 64, no. 12. pp. 1292–1309, 2012, doi: 10.1016/j.addr.2012.01.016.

[36] A. R. Rezende, P. J. Bartolo, A. Mendes, and R. M. Filho, "Rheological Behavior of Alginate Solutions for Biomanufacturing," *J. Appl. Polym. Sci.*, vol. 113, no. 5, p. 3866−3871, 2009, doi: 10.1002/app.

[37] I. P. Shanura Fernando, D. Kim, J. W. Nah, and Y. J. Jeon, "Advances in functionalizing fucoidans and alginates (bio)polymers by structural modifications: A review," *Chem. Eng. J.*, vol. 355, no. May 2018, pp. 33–48, 2019, doi: 10.1016/j.cej.2018.08.115.

[38] K. Y. Lee and D. J. Mooney, "Alginate: Properties and biomedical applications," *Prog. Polym. Sci.*, vol. 37, no. 1, pp. 106–126, 2012, doi: 10.1016/j.progpolymsci.2011.06.003.

[39] M. Dalheim, J. Vanacker, M. A. Najmi, F. L. Aachmann, B. L. Strand, and B. E. Christensen, "Efficient functionalization of alginate biomaterials," *Biomaterials*, vol. 80, pp. 146–156, 2016, doi: 10.1016/j.biomaterials.2015.11.043.

[40] W. Wei *et al.*, "Advanced hydrogels for the repair of cartilage defects and regeneration," *Bioact. Mater.*, vol. 6, no. 4, pp. 998–1011, 2021, doi: 10.1016/j.bioactmat.2020.09.030.

[41] DIVYA NATARAJ and N. REDDY, "Chemical Modifications of Alginate and Its Derivatives," *Int. J. Chem. Res.*, vol. 4, no. 1, pp. 1–17, 2019, doi: 10.22159/ijcr.2020v4i1.98.

[42] N. O. Dhoot, C. A. Tobias, I. Fischer, and M. A. Wheatley, "Peptide-modified alginate surfaces as a growth permissive substrate for neurite outgrowth," *J. Biomed. Mater. Res. - Part A*, vol. 71, no. 2, pp. 191–200, 2004, doi: 10.1002/jbm.a.30103.

[43] G. Auriemma, P. Russo, P. Del Gaudio, C. A. García-González, M. Landín, and R. P. Aquino, "Technologies and formulation design of polysaccharide-based hydrogels for drug delivery," *Molecules*, vol. 25, no. 14, pp. 1–36, 2020, doi: 10.3390/molecules25143156.

[44] S. I. Somo *et al.*, "Synthesis and evaluation of dual crosslinked alginate microbeads," *Acta Biomater.*, vol. 65, no. January, pp. 53–65, 2018, doi: 10.1016/j.actbio.2017.10.046.

[45] J. Simfukwe, R. E. Mapasha, A. Braun, and M. Diale, "Biopatterning of Keratinocytes in Aqueous Two-Phase Systems as a Potential Tool for Skin Tissue Engineering," *MRS Adv.*, vol. 357, no. May, pp. 1–8, 2017, doi: 10.1557/adv.201.

[46] S. Bubenikova *et al.*, "Chemoselective cross-linking of alginate with thiol-terminated peptides for tissue engineering applications," *Carbohydr. Polym.*, vol. 88, no. 4, pp. 1239–1250, 2012, doi: 10.1016/j.carbpol.2012.01.089.

[47] "Arginylglycylaspartic acid - Wikipedia."

https://en.wikipedia.org/wiki/Arginylglycylaspartic_acid (accessed Jan. 14, 2021).

[48] J. A. Rowley, G. Madlambayan, and D. J. Mooney, "Alginate hydrogels as synthetic extracellular matrix materials," *Biomaterials*, 1999, doi: 10.1016/S0142-9612(98)00107-0.

[49] H. W. Ooi, C. Mota, A. Tessa Ten Cate, A. Calore, L. Moroni, and M. B. Baker, "Thiol-Ene Alginate Hydrogels as Versatile Bioinks for Bioprinting," *Biomacromolecules*, vol. 19, no. 8, pp. 3390–3400, 2018, doi: 10.1021/acs.biomac.8b00696.

[50] K. D. He, S.L., Zhang, M., Geng, Z.J.,&Yao, "Preparation and Characterization of Partially Oxidized Sodium Alginate," *Chinese J. Appl. Chem.*, 2005.

[51] A. Lueckgen, D. S. Garske, A. Ellinghaus, D. J. Mooney, G. N. Duda, and A. Cipitria, "Enzymatically-degradable alginate hydrogels promote cell spreading and in vivo tissue infiltration," *Biomaterials*, vol. 217, no. May, p. 119294, 2019, doi: 10.1016/j.biomaterials.2019.119294.

[52] "Electron Microscopy | Scanning Electron Microscopy | Thermo Fisher Scientific - ES." https://www.thermofisher.com/es/es/home/materials-science/learning-center/applications/sem-electrons.html (accessed Jan. 18, 2021).

[53] Bruker Corporation, *FTIR Basics – Principles of Infrared Spectroscopy*. 2019.

[54] S. K. Sharma, D. S. Verma, L. U. Khan, S. Kumar, and S. B. Khan, "Fourier transform infrared spectroscopy: Fundamentals and application in functional groups and nanomaterials characterization," in *Handbook of Materials Characterization*, no. September, 2018, pp. 317–344.

[55] "Rheology 101 – Learning the Basics." https://www.azom.com/article.aspx?ArticleID=16985 (accessed Jan. 18, 2021).

[56] "It's the Rheo Thing: Viscoelasticity: It's Not Just for Polymers Anymore." http://www.rheothing.com/2012/08/viscoealsticity-its-not-just-for.html (accessed Jan. 21, 2021).

[57] B. Manjula, K. Varaprasad, R. Sadiku, and K. M. Raju, "Preparation and Characterization of Sodium Alginate-Based Hydrogels and Their In Vitro Release Studies," *Adv. Polym. Technol.*, vol. 32, no. 2, p. n/a-n/a, Jun. 2013, doi: 10.1002/adv.21340.

Annex A

Details of the quantities of products used for alginate modification/functionalization

A1. Quantities of chemicals used to modify alginate with norbornene

MES buffer	Alginate	COOH activated	EDC	NHS	Norbornene
50 mL	500 mg	5 %	25 mg	7.5 mg	33.4 µL
		20 %	100 mg	30 mg	128.5 µL
		50 %	250 mg	75 mg	334.9 µL

A2. Quantities of chemicals used to functionalized alg-norb with RGD peptides

COOH activated	LAP (100mM)	Peptide (1g/L)
5 %	47.5 µL	100 µL = 1mg RGD/g alg
20 %	190 µL	
50 %	475 µL	

A3. Quantities of chemicals used to modify alginate with PDEA

MES buffer	Alginate	COOH activated	EDC	NHS	PDEA
50 mL	500 mg	10 %	50 mg	15 mg	58 mg